SUPPLEMENTAL MATERIAL

Supplemental Methods

Animals.

Tamoxifen (4-OHT: 4-hydroxytamoxifen)-inducible EC-specific ERK5 KO mice (Inducible ERK5-EKO mice) were generated by crossing mice expressing tamoxifen-inducible Cre-recombinase CreER^{T2} under the regulation of the vascular endothelial cadherin (VE-Cad) promoter[1] (kindly gifted from Dr. Iruela-Arispe) with a conditional KO line of ERK5[2]. The latter mice have loxP sites inserted at the 3' and 5' ends of exon 4 in the *Erk5* gene[2].

Rat wild type p90RSK1 cDNA containing the Kozak and Flag sequences from pCMV-Taq2b were cloned into the NotI/XhoI sites of the plasmid Z/EG, which consists of pCAGGS promoter, directing expression of a *loxP*flanked bgeo (*lacZ*/neomycin-resistance) fusion gene and three SV40 polyadenylation sequences[3]. We gave these constructs to the University of Rochester Transgenic Facility, and we have obtained five founders of these mice. Genotype of mouse pups was confirmed by PCR analysis of tail clipping using standard procedure. To induce deletion of the *Erk5* gene or expression of wild type *p90RSK1* gene, 4-week old heterozygous VE-Cad-CreER^{T2}/*Erk5*$^{flox/-}$ (Inducible ERK5-EKO$^{+/-}$) or homozygous VE-Cad-CreER^{T2}/*Erk5*$^{flox/flox}$ (Inducible ERK5-EKO$^{-/-}$), or VE-Cad-CreER^{T2}/WT-p90RSK$^{flox/-}$ mice were injected with peanut oil, with or without 2 mg of 4-OHT for 5 consecutive days. The diabetogenic Akita mutation (C96Y) in the insulin 2 genes of the C57BL/6 strain were purchased from Jackson Laboratory. C57BL/6 wild type mice (Taconic, Hudson, NY) fed standard chow diet were used for en face study. For atherosclerosis study using Ang II infusion model, male ApoE-KO mice were obtained from the Jackson Laboratory (Bar Harbor, Me) and bred in house with a specific,

pathogen-free environment. Mice received Ang II via an osmotic minipump for 28 days. During that time, mice were fed standard chow diet. For atherosclerosis using high cholesterol diet (HCD), inducible ERK5-EKO-LDLR$^{-/-}$ mice were fed with HCD for 16 weeks. Food and tap water were administrated ad libitum. All mice of C57BL/6 wild type and ApoE$^{-/-}$ male mice were used between the ages of 6 and 9 weeks. All experiments were approved by the University of Rochester Institutional Animal Care and Use Committee.

Antibodies and reagents.

Antibodies were purchased from the following vendors: anti-p90RSK1 (C-21, #SC-231), anti-p90RSK2 (E-1, # sc-9986), anti-VP16 (#SC-7546) and anti-VCAM-1 (SC-8304) from Santa Cruz (Santa Cruz Biotechnology, CA); anti-phospho-p90RSK (Ser380, # 9341), anti-phospho-ERK5 (Thr218/Tyr220, #3371L), anti-ERK5 (#3372), and anti-ERK1/2 (#9102) from Cell Signaling (Cell Signaling Technology Inc, Danvers, MA); anti-tubulin (T-5168) and anti-Flag (# F-3165) from Sigma (Sigma, St. Louis, MO); and anti-eNOS (#610299) and anti-VE-cadherin (#555289) from BD Transduction Laboratory (Pharmingen, San Diego, CA), anti-Eselectin (# 3631-100) from Bio Vision (CA 94043). Hydrogen Peroxide was purchased from Sigma (#216763). GST fused active recombinant full-length rat RSK1 (Cat # 14-479) was purchased from Millipore (Millipore, Billerica, MA).

Generation of human anti-phospho-ERK5-S496 antibody.

A peptide corresponding to amino acids 486-506 of mouse ERK5 (SLRSRLRDGPS*APLEAPEPRK) was synthesized (Peptibody Inc. 2216 Mermans Rd Charlotte, NC 28270, US) with an amino-terminus biotin in both phosphorylated and unphosphorylated forms. A human anti-phospho-ERK5-S496 single-chain Fv (scFv) was

generated against the phospho-peptide by phage display[4] with a naïve, human phage display library constructed from peripheral blood lymphocytes[5,6]. The phospho-peptide was bound to streptavidin-coated immunowells (Pierce) and the phage library was enriched for three rounds, switching to neutravidin-coated wells for the second round to avoid isolating anti-streptavidin scFvs. Individual clones from the second and third rounds were screened by phage ELISA and a clone reactive with phosphorylated peptide, but not with un-phosphorylated peptide, was identified. The scFv was sequenced, re-amplified and cloned into a human immunoglobulin heavy chain expression[7] vector modified by deletion of the CH1 domain to produce an scFv-Fc fusion protein. This plasmid was transiently transfected into HEK293T cells and the medium was harvested every three days. The culture supernatants from three harvests were combined, and the scFv was purified on an Aspire protein G tip (Thermo-Fisher). The protein was eluted from the tip and dialyzed into PBS and used for Western blotting experiments. The fusion protein was detected with anti-human IgG antibodies.

Plasmid and adenovirus vector construction.

Kinase dead rat RSK-1 (Genebank NM031107) with K94A/K447A mutations was created using a QuikChange site-directed mutagenesis kit (STRATAGENE, Agilent Technologies, Santa Clara, CA)[8]. Mouse ERK5 and a constitutively active form of MEK5α (CA-MEK5α) were cloned as previously described[9]. VP16 wild type and truncated forms of mERK5a were created by inserting the mouse wild type and truncated mERK5a isolated from pcDNA3.1-mERK5a into BamHI and NotI sites of the pACT vector. Glutathione S-transferase (GST)-ERK5 was created by cloning PCR-amplified DNA fragments corresponding to the different ERK5 regions into the EcoRI-XhoI sites of the pGEX-KG vector (Amersham Biosciences, GE Healthcare Biosciences,

Pittsburgh, PA). ERK5 constructs with various point mutations were created using the QuikChange site-directed mutagenesis kit (Stratagene). A reporter gene encoding KLF2 promoter (-924 ~ + 14) was a kind gift from Dr. Jerry B. Lingrel (University of Cincinnati, Cincinnati, OH). Human eNOS promoter (eNOS-Luc, -1197) was a gift from Dr. David Gardner (University of California, San Francisco, CA). For adenovirus preparation, DN-p90RSK construct was cloned into an AdEasy-CMV system (QBIOGen, Carlsbad, CA) with Sal*I* and Hind*III* restriction enzymes[8]. All constructs were verified by DNA sequencing. Adenovirus vector containing β-galactosidase (Ad-LacZ) was used as a control virus.

Cell Culture and transfection.

Human umbilical vein ECs (HUVECs) were obtained from collagenase digested umbilical cord veins [10] and collected in M200 medium supplemented with LSGS (Cascade Biologics Inc., Portland, OR) and 2% fetal bovine serum (FBS) (Atlanta Biologicals Inc., Lawrenceville, GA). HUVECs were cultured in 0.2% gelatin pre-coated dishes. For transient expression experiments, 70 to 80% confluent cells were transfected with cDNA using Opti-MEM containing Plus-Lipofectamine as we previously described [11]. After 4 hrs of transfection, Opti-MEM was replaced with the complete M200 medium. HeLa cells were maintained in DMEM (GIBCO, Carlsbad, CA) supplemented with 10% FBS, 50 units/ml penicillin, and 50 μg/ml streptomycin.

Analysis of metabolic parameters

For analysis mice were anesthetized and blood samples were collected from the abdominal artery. Plasma was prepared and plasma total cholesterol, HDL, and non-HDL (LDL and VLDL) concentrations were measured enzymatically using commercially available kits (Abcam,

ab65390). The assays were performed in accordance with the manufacturer's instructions. For glucose tests, mice fasted overnight were given one i.p. injection of glucose (2 mg/g body weight) in PBS, and tail blood was collected before (time 0) and at indicated times after injection for measurement of glucose (Glucometer Elite; Bayer).

Atherosclerosis and AAA model

Using osmotic minipumps[12] (model 1004; Alzet Osmotic pumps) implanted subcutaneously, 3 groups of mature ApoE-KO male mice (8-12 weeks), each group consisting of 10-18 mice, received saline, Ang II (Calbiochem, 670 ng/kg/min for atherosclerosis), or Ang II (1000 ng/kg/min for AAA) for 4 weeks. In addition, to assess the role of p90RSK activation, some mice were treated with FMK-MEA (80 mg/Kg body weight/day) by interperitoneal injections for 21 constitutive days 7 days after Ang II infusion was started. We observed animals daily, and in the case of premature sudden death, we performed necropsy to determine the cause of death. Determining the plaque area of the aorta using Oil Red O staining of en face mounts and paraffin-embedded aortic valves sections were used for assessment of atherosclerosis. AAA was defined as greater than or equal to 50% enlargement of the maximal abdominal aorta diameter.

Tissue preparation, histology, and quantification of the lesion sizes.

Mice were sacrificed 28 days following implantation of osmotic minipumps. Animals of 6-9 weeks of age were euthanized by CO_2 inhalation. The arterial tree was perfused via the left ventricle with saline containing heparin (40 USPU/mL), followed by paraformaldehyde (4%, pH 7.3) in PBS for 10 min. We exposed the full-length of the aorta-to-iliac bifurcation and dissected carefully from any surrounding tissues, and opened the aortas along the ventral midline. En face

preparations of the aortas were washed in distilled water, dipped in 70% isopropyl-alcohol, and stained for 40 min in 0.16% Oil-Red-O dissolved in 70% isopropyl-alcohol/0.2 mol/l NaOH. Aortic images were captured with a digital camera mounted on a Leica stereomicroscope and analyzed using Adobe Photoshop Extended software. The stained plaque areas were quantified blindly using ImageJ 1.45 (available as freeware from http://rsbweb.nih.gov/ij/). The percentage of lesion area from full-length of the aorta-to-iliac bifurcation (Fig. 3F, and 8A) or ascending area, from the arch to the last diaphragm (Fig. 8B) was calculated as total lesion area divided by total surface area. To examine the atherosclerotic lesions in the aortic valve area using histology, the heart and aortic sinus area was dissected from full-length of the aorta and then embedded in paraffin. Serial sections (5 μm) were taken throughout the entire aortic valve area and stained with hematoxylin and eosin (H&E) to assess the quantification of atherosclerotic plaque. To quantify the extent of intimal surface covered by grossly discernible lesions, image analysis was performed with ImageJ 1.45. The percentage of lesion area was calculated as total lesion area divided by total surface area.

Isolation of mouse ECs from lung tissue (MECs).

Method for isolation of MECs was modified from published protocols [13]. Briefly, the lung from each mouse was harvested, minced finely with scissors, and then digested in 15 ml collagenase (2 mg/ml; Worthington Biochemicals Corp., Lakewood, NJ, Cat # 4177) at 37^0C for 45 min. The suspension was then triturated 15 -20 times using a 20 ml syringe attached to a cannula, avoiding frothing, and was filtered through a 70 μm cell strainer. The crude cell preparation was pelleted and resuspended in cold DPBS with Ca/Mg (HyClone, HyClone Laboratories Inc., Logan, UT, Cat # SH30264.01) and 0.1% BSA (Sigma-Aldrich, # A9576) and the cell

concentration was adjusted to $3x10^7$ cells/mL. Dynabeads were conjugated with sheep anti-rat IgG (Invitrogen; Cat # 110.35), and then incubated with rat anti-mouse PECAM-1 (Pharmingen, San Diego, CA, Cat # 553370) according to the manufacturer's instructions. The cell suspension was incubated with PECAM-1-coated beads (35 μl beads/mL cell suspension) at room temperature for 30 min with end-over-end rotation. Using a magnetic separator stand (Promega, Madison, WI, Cat # Z5410), cells bound to the beads were recovered, washed with DMEM containing 20% FBS, suspended in 6 mL complete culture medium [DMEM containing 20% FBS, supplemented with 100 μg/mL porcine heparin, 100 μg/mL EC grow supplement (ECGS; Biomedical Technologies Inc., Stoughton, MA), nonessential amino acids, sodium pyruvate, and antibiotics at standard concentrations], and then plated in a 0.2% gelatin-coated 6 cm dish. Once the cells reached 70-80% confluence, they were detached with trypsin-ethylenediaminetetraacetate (EDTA) to generate single-cell suspension, pelleted, and then resuspended in 2 mL DPBS with Ca/Mg and 0.1% BSA and incubated with PECAM-1-coated beads (35 μl beads/mL cell suspension) at RT for 15 min with rotation. The bound cells were washed and plated in complete culture medium. Cells were used for experiments at passages 3.

Real-time RT-PCR.

MECs were isolated from mouse lungs as described previously. At passage 3, cells were seeded at ~ 30% density into 6-well-plate and left to grow in the presence of DMEM low glucose supplemented with 10% FBS. Once confluent, cells were pretreated with vehicle or 10 μM of FMK-MEA for 3 hrs, followed by stimulation with either HG/low H_2O_2 or Mannitol/low H_2O_2 as a control. Then, total RNA was isolated using RNeasy Plus Mini Kit (Cat. # 74134, QIAGEN Sciences, Maryland 20874, US) according to the manufacturer's instruction. During this process,

genomic DNA contamination was eliminated by gDNA Eliminator column, which is included in the Kit. First strand cDNA synthesis was done in 50 μL reaction using 2 μg of purified RNA, 5 μL 10X buffer, 11 μL $MgCl_2$, 10 μL dNTPs, 2.5 μL random hexamer, 1.25 μL oligo dT, 1 μL RNAse inhibitor, and 0.75 μL reverse transcriptase enzyme (TaqMan Reverse Transcription Reagents, N808-0234, made for Applied Biosystems by Roche Molecular systems, Inc., Branchburg, New Jersey, US). Target cDNA levels were quantified by real-time RT-PCR using a MyiQ™2 Optics Module (Bio-Rad Laboratories, Inc.). Each reaction mixture (20 μL) contained cDNA synthesized from 20 ng of total RNA, 10 μL of iQ™SYBR Green Supermix (Bio-Rad Laboratories, Inc.), 0.5 μmol/L of each primer. The real-time PCR protocol consisted of the initial step at 95^0C for 3 min, followed by 40 cycles: 95^0C for 10 sec and annealing at 55^0C for 30 sec. The ΔΔCt method was used to calculate the fold change in mRNA expression: ΔCt = Ct (target gene) – Ct (housekeeping gene), ΔΔCt = ΔCt (treatment) - ΔCt (control), fold change = $2^{(-\Delta\Delta Ct)}$. Primer sequences are as follows: mouse VCAM-1 forward: 5'-TGA CAA GTC CCC ATC GTT GA-3' and reverse: 5'-ACC TCG CGA CGG CAT AAT T-3'[14]; Mouse GAPDH forward: 5'-TGG CAA AGT GGA GAT TGT TGC C-3' and reverse: 5'-AAG ATG GTG ATG GGC TTC CCG-3'; Mouse KLF2 forward: 5'-ACC AAG AGC TCG CAC CTA AA-3' and reverse: 5'-GTG GCA CTG AAA GGG TCT GT-3'. Mouse eNOS forward: 5'-TCT ACC GGG ACG AGG TAC TG-3' and reverse: 5'-CTG TCC TCA GGA GGT CTT GC-3'[15]. Mouse E-selectin forward: 5'-ATC TGG TGG CGA TTC AGA AC- 3' and reverse: 5'-TGT TGT TTG GTT CAC CTG GA-3'[16].

Mammalian one- and two-hybrid analyses and transfection of cells.

Sub-confluent HUVECs plated in 12-well plates were transfected using Opti-MEM (Invitrogen, Carlsbad, CA) containing Plus-Lipofectamine mixture with the pG5-luc vector and various pBIND and pACT plasmids (Promega, Madison, WI), as indicated, for 4 hrs. Cells were then washed, and complete M200 medium supplemented with LSGS and 2% FBS was added. The pG5-luc vector contains five Gal4 binding sites upstream of a minimal TATA box, which in turn, is upstream of the firefly luciferase gene. pBIND containing Gal4 was fused with p90RSK, and pACT containing VP16 was fused with either full length ERK5 or ERK5 fragments, as indicated. Since pBIND also contains the Renilla luciferase gene, expression and transfection efficiencies were normalized to the Renilla luciferase activity. Cells were harvested 24 hrs after transfection unless otherwise indicated, and luciferase activity was assayed using a dual-luciferase reporter system (Promega, Madison, WI) using a TD-20/20 Luminometer (Turner Designs, Sunnyvale, CA). Transfections were performed in triplicate, and each experiment was repeated at least three times. For the one-hybrid analysis, HUVECs were transfected with the pG5-luc vector and Gal4-fused ERK5 constructs in the presence of pcDNA3.1-CA-MEK5α or pcDNA3.1 as a control. After 4 hrs of transfection, Plus-Lipofectamine/Opti-MEM was replaced by supplemented M200 medium, and then cells were incubated for another 8 hrs before being exposed to H_2O_2, D-glucose (25 mM), or mannitol (25 mM) for indicated lengths of time. Transfections were performed in triplicate, and each experiment was repeated at least twice.

KLF2 promoter activity.

Sub-confluent HUVECs were transfected with Flag-ERK5, a reporter gene encoding KLF2 promoter (-924 ~ + 14), pRL-CMV (as a luciferase control reporter vector), and pcDNA3.1-CA-MEK5, or pcDNA3.1 as a control vector. After 4 hrs of transfection, Plus-Lipofectamin/Opti-

MEM was replaced by supplemented M200 medium and cells were incubated for another 4 hrs before being treated with FMK. Then, the cells were treated with FMK (10 μM) for 3 hrs prior to H_2O_2 stimulation for 24 hrs. KLF2 promoter luciferase activity was assayed using a dual-luciferase reporter assay system. The experiment was repeated three times.

Flow stimulation.

Confluent HUVECs cultured in 100-mm dishes were exposed to laminar flow as we previously described[11] in a cone and plate viscometer placed in a cell incubator with 5% CO_2 and at 37^0C for 24 hr (shear stress = 12 dyn/cm^2).

In vitro kinase assay of ERK5.

ERK5 kinase activity was measured by auto-phosphorylation assay as we described previously[17].

Immunoprecipitation.

Cell extracts were prepared in modified radioimmunoprecipitation assay 1 (RIPA) buffer [50 mM Tris-HCl, pH 7.4; 150 mM NaCl; 1 mM EDTA; 1% Nonidet P-40; 0.1% sodium dodecyl sulfate (SDS); 0.25% Sodium Deoxycholate; 1:200-diluted protease inhibitor cocktail (Sigma, St. Louis, MO); 1 mM PMSF; and 10 mM NEM]. Immunoprecipitation with a mouse monoclonal anti-Flag, or a polyclonal rabbit anti-ERK5 was performed as described previously[18]. Bound proteins were released in 2× SDS sample buffer, resolved by SDS-polyacrylamide gel electrophoresis, transferred onto a Hybond enhanced chemiluminescence nitrocellulose membrane (GE Healthcare, Piscataway, NJ, USA), and visualized by using the enhanced

chemiluminescence detection reagent (PerkinElmer, Shelton, CT, USA) according to the manufacturer's instruction.

Bodipy-FMK Rsk1/2 occupancy assay using heart lysates from mice treated with FMK-MEA.

Frozen heart tissues from mice that were injected intraperitoneally with FMK-MEA (Fig.S12) (0, 15, 35 and 50 mg/kg in PBS) were thawed on ice in the presence of 2 mL PBS containing protease (Complete, Roche) and phosphatase (Cocktail I and II, Sigma) inhibitors. The tissues were kept on ice and were homogenized three times for 30 sec at 13,500 rpm with an electric tissue Tearor (Janke & Kunkel/IKA T25-Ultra-Turrax Homogenizer). The homogenates were transferred to clean 4 mL ultracentrifuge tubes (Beckman) and were clarified by centrifugation at 30,000 x g for 60 min (Beckman Coulter Optima TLX Ultracentrifuge; TLA-100.3 rotor). Next, 250 μL of the clarified lysate (normalized to 2.5 mg/mL) derived from the vehicle-treated mouse was pre-treated with FMK-MEA (3 μM) for 1 hour at room temperature, and then reacted with bodipy-FMK (5 μM) for 1 hour at room temperature. This sample was a control for the labeling specificity of bodipy-FMK in the heart tissue lysates. Separately, 250 μL each of the clarified lysates (from mice treated with 0, 15, 35 and 50 mg/kg FMK-MEA; normalized to 2.5 mg/mL) were reacted with bodipy-FMK (5 μM) for 1 hour at room temperature (without FMK-MEA pre-treatment). Following the bodipy-FMK treatment, each sample (270 μL total) was diluted with 730 μL ice cold PBS + 1% NP40. Immunoprecipitation was performed using 4 μg Rsk2 antibody (E-1, sc-9986 mouse monoclonal antibody, Santa Cruz Biotechnology) for 3 hr at 4°C, followed by overnight incubation at 4°C with 50 μL of Protein G Sepharose beads (GE Healthcare). The beads were washed three times for 10 min with 500 μL PBS + 1% NP40,

pelleted and resuspended in 50 μL Laemmli sample buffer. A second immunoprecipitation step was performed with the remaining supernatants using 4 μg Rsk1 antibody (C-21, sc-231 rabbit polyclonal antibody, Santa Cruz Biotechnology) for 3 hr at 4˚C, followed by overnight incubation at 4˚C with 50 μL of Protein G Sepharose beads (GE Healthcare). The beads were washed three times for 10 min with 500 μL PBS + 1% NP40, pelleted and resuspended in 50 μL Laemmli sample buffer. The samples were resolved on 10% SDS-PAGE and detected by in-gel fluorescence scanning with a Typhoon 9400 flatbed laser-induced scanner, followed by transfer to nitrocellulose membrane and western blot detection with antibodies against RSK1 and RSK2.

***En Face* immunohistochemistry.**

S-flow areas within the aorta were chosen based on published and generally accepted anatomical locations where such flow patterns are known to occur[19, 20]. For example, an s-flow area is located in the greater curvature area or marked as a low probability region for lesion formation[19], which is also known as a high wall shear stress area[19, 20]. EC shape outlined by anti-VE-cadherin staining was also used to identify s-flow area (elongated cell shape) and disturbed flow areas (irregular cell shape). C57BL/6 wild type mice (Taconic, Hudson, NY) were fed standard chow. Animals of 6-9 weeks of age were euthanized by CO_2 inhalation. The arterial tree was perfused via the left ventricle with saline containing heparin (40 USPU/mL), followed by 4% paraformaldehyde in PBS for 10 min. After adipose tissues were removed aortas were cut open longitudinally and permeabilized with PBS containing 0.1% Triton X-100 and blocked by TBS containing 10% goat serum and 2.5% Tween-20 for 30 min. Aortas were incubated with (animal-rabbit) anti-p90RSK or (animal-rabbit) anti-phospho-p90RSK with (animal-rat) anti-VE-cadherin in the blocking solution overnight. After rinsing with PBS, anti-rabbit IgG and

anti-rat IgG (1:1000 dilution, Alexa Fluor 546 or 488 tagged, respectively, Molecular Probes, Carlsbad, CA) were applied for 1 hr at RT. Images were observed using a confocal laser scanning microscope (Olympus, Tokyo, Fluoview 300) equipped with krypton/argon/HeNe laser lines and 20X (N.A. 0.70), 40X (N.A.1.0), and 60X (N.A.1.4) objectives. All images were collected using the same confocal setting. p90RSK and phospho-p90RSK expression in ECs of aortic arch of wild type was quantified using Adobe Photoshop by assessing fluorescence intensity after background fluorescence was subtracted. All animal procedures were performed with the approval from the University Committee on Animal Resources, University of Rochester.

Leukocyte rolling assay and vessel diameter measurements

Intravital microscopy was performed as previously described [21]. Leukocytes were labeled by intravenous injection of rhodamine 6G (50 μl of 0.05% solution in H_2O). Mice were anesthetized with ketamine (80 mg/kg) and xylazine (13 mg/kg). The mesentery was exteriorized, and an area containing target venules (120–150 μm in diameter) was selected and mounted on an inverted fluorescent microscope (Nikon, ECLIPSE Ti) with a 37°C stage warmer. Images of leukocyte rolling were video-recorded by electron-multiplying CCD camera (*QuantEM,* 512SC). Leukocyte rolling on the endothelium was quantified for 2 min (NIS elements, Nikon). Leukocyte rolling flux (Number of rolling leukocytes passing a perpendicular line placed across the observed vessel in one minute) and velocity, leukocyte adhesion (leukocytes showing no movement during 2 min recording), and venular wall shear rate were determined as previously described[22]. Venule diameter was measured by direct observation using image analysis software as described previously[23]. Briefly, the venules were induced by the superfusion of 30 μL of cumulative doses of acetylcholine (10 nM to 10 μM), subsequent

recordings were performed for 2 min between each dose, followed by 10 min equilibration to the 10 μM phenylephrine. Vessel tone was analyzed by direct measuring of diameter using image analysis software (NIS elements, Nikon).

Ambit/DiscoverX platform screening (Table S1)

"Kinomescan" binding assays[24, 25] (www.kinomescan.com) were performed by Ambit (now DiscoverX), and the following description is derived from the study report provided by Ambit/DiscoverX. The Ambit kinase screening platform is based on a competition binding assay that quantitatively measures the ability of a compound to compete with an immobilized, active-site directed ligand. The assay is performed by combining three components: DNA-tagged kinase; immobilized ligand; and a test compound (FMK-MEA, 1 μM). The ability of the test compound to compete with the immobilized ligand is measured via quantitative PCR of the DNA tag. For most assays, kinase-tagged T7 phage strains were grown in parallel in 24-well blocks in E. coli. E. coli were grown to log-phase and infected with T7 phage from a frozen stock (multiplicity of infection = 0.4) and incubated with shaking at 32°C until lysis (90-150 minutes). The lysates were centrifuged (6,000 x g) and filtered (0.2μm) to remove cell debris. The remaining kinases were produced in HEK-293 cells and subsequently tagged with DNA for qPCR detection. Streptavidin-coated magnetic beads were treated with biotinylated small molecule ligands for 30 minutes at room temperature to generate affinity resins for kinase assays. The liganded beads were blocked with excess biotin and washed with blocking buffer (SeaBlock (Pierce), 1 % BSA, 0.05 % Tween 20, 1 mM DTT) to remove unbound ligand and to reduce non-specific phage binding. Binding reactions were assembled by combining kinases, liganded affinity beads, and test compounds in 1x binding buffer (20 % SeaBlock, 0.17x PBS, 0.05 %

Tween 20, 6 mM DTT). FMK-MEA was prepared as a 40x stock in 100% DMSO and directly diluted into the assay. All reactions were performed in polypropylene 384-well plates in a final volume of 0.04 ml. The assay plates were incubated at room temperature with shaking for 1 hour and the affinity beads were washed with wash buffer (1x PBS, 0.05 % Tween 20). The beads were then re-suspended in elution buffer (1x PBS, 0.05 % Tween 20, 0.5 μm non-biotinylated affinity ligand) and incubated at room temperature with shaking for 30 minutes. The kinase concentration in the eluates was measured by qPCR.

Expanded discussion

We did not show data on diabetes-enhanced atherosclerosis in this study, although our study strongly suggested mechanistic correlation between diabetes and atherosclerosis. The main aim of our study was not on determining the mechanism of diabetes-mediated acceleration of atherosclerosis, but rather we focused on the following two goals: 1) to determine the role of the p90RSK-ERK5 module in endothelial dysfunction, and 2) to investigate the role of p90RSK activation (which causes endothelial dysfunction) on atherosclerosis formation. Since we have found that the diabetes mouse models (STZ and Akita) exhibit the most reproducible and reliable endothelial dysfunction and also have high pathological significance, we used these models in this study and found the important role of the p90RSK-ERK5 module in endothelial dysfunction in vivo, which presumably leads to atherosclerosis in these animals[26]. In addition, we found increased p90RSK activation in the disturbed flow area, which is a pro-atherogenic area in aortic arch (Heo KS, Abe J, unpublished data). These data suggest a role of p90RSK activation on athereosclerosis formation, and indeed we found that the inhibition of p90RSK activation by FMK-MEA significantly reduced atherosclerosis formation and that depletion of ERK5 accelerated it. We believe that these data provide strong evidence for the key role of the p90RSK-ERK5 module in endothelial dysfunction and atherosclerosis formation.

Limitation of this study

As shown in Fig.4A-E, we found that p90RSK activation was significantly increased in STZ treated mice, suggesting that p90RSK was, indeed, activated in the DM model in vivo. However, HG 25 mM alone could not activate p90RSK activation in HUVECs *in vitro*. Although we found that 100 μg/mL AGE could activate p90RSK in HUVECs (Fig. S2D, E), it will be

important to determine the major physiological stimulus and mechanism of p90RSK activation in DM condition. In addition, although the role of this module on endothelial dysfunction in vivo was further demonstrated by eliminating the beneficial effect of FMK-MEA in EC-specific ERK5 depletion mice, the role of endothelial ERK5 in p90RSK-mediated atherosclerosis formation remains unclear. To prove this we will perform p90RSK inhibition in endothelial specific ERK5-KO mice and detect atherosclerosis formation in our future study. It will also be necessary to create a model of atherosclerosis with the DM background and use it to prove the role of the p90RSK-ERK5 module in DM-mediated acceleration of atherosclerosis.

Supplemental Tables

Table S1: Specificity of FMK-MEA

To show the specificity of FMK-MEA, we used the Ambit/DiscoverX platform to measure its apparent binding constant (Kd) to 443 human kinases. We found that all kinases except RSK1/4 CTD bound with Kd >> 1 μM. This profiling experiment was carried out in vitro against recombinant kinase domains. It is well known that the vast majority of kinase inhibitors shows potency shifts of 10-100 fold when comparing in vitro to cellular assays, because the inhibitors must compete with high intracellular concentrations of ATP (> 1 mM)[27]. Given this lower limit for the apparent Kd, it is unlikely that the kinases would be significantly inhibited in cells at 10 μM, especially given the high intracellular concentration of ATP (> 1 mM) as described previously[27].

Supplemental Figure Legends

Figure S1. Transduction of dominant negative ERK5 (Ad-DN-ERK5) could not inhibit H_2O_2-induced p90RSK activation, and the role for H_2O_2-induced p90RSK activation in ERK5 transcriptional activity and the KLF2 and eNOS promoter activity.

(A, B) Following transduction with either Ad-LacZ or Ad-DN-ERK5 for 24 hours, HUVECs were treated with 200 μM H_2O_2 or vehicle for indicated times. p-p90RSK, p90RSK, p-ERK5, ERK5, p-ERK1/2, and tubulin expressions were detected by Western blotting in the total cell lysates with each specific antibody (A). Quantification of p90RSK phosphorylation was expressed as the relative ratio compared with p90RSK (2^{nd} from top) bands. Results were normalized to the lowest phosphorylation level within each set of experiments, and statistical significance was determined by comparing the average level of the control group with that of each experimental data point. Experiments were carried out in triplicates using 3 different batches of H_2O_2-stimulated HUVECs (mean ± SEM, n = 3, $^{**}P < 0.01$ compared to control) (B). (C) HUVECs were co-transfected with plasmids encoding Gal4-ERK5 and the Gal4-responsive luciferase reporter pG5-Luc. Cells were also transfected with an empty vector or CA-MEK5α as indicated. After 16 hrs cells were serum starved by replacing completed M200 medium by M200 medium without any supplement. One hour later, cells were treated with various concentrations of FMK-MEA as indicated for 30 min, followed by stimulation with 200 μM H_2O_2 for 16 hrs. Finally, ERK5 transcriptional activity were assayed as described in Fig. 1E. (mean ± SEM, n = 3, $^{*}P < 0.05$) (D) HUVECs were co-transfected with either DN-p90RSK vector or empty vector, and the KLF2 promoter with luciferase (left) or the eNOS promoter with luciferase (right) reporter gene. Eight hours after transfection, cells were treated with or without H_2O_2 (200 μM) and exposed to s-flow or no flow. Luciferase activities were assayed 24 hrs after

the flow stimulation. Data are representative of three independent experiments (mean ± SEM, n = 3, *p < 0.05, **P < 0.01).

Figure S2. The role of p90RSK activation in combined effects of high glucose and low dose H_2O_2 and advanced glycation end products (AGE)-induced reduction of ERK5 transcriptional activity.

(A, B) A **c**ombination of high glucose (25 mM) and low dose H_2O_2 (20 μM) increases p90RSK activation. HUVECs were stimulated with low dose H_2O_2 alone or with the combination of high glucose and low dose H_2O_2 for indicated times. p90RSK activation and p90RSK expression were detected by Western blotting with anti-phospho-p90RSK and anti-p90RSK, respectively (A). Phosphorylation levels of p90RSK were densitometrically determined (mean ± SEM, n = 3, *p < 0.05 compared with control 0 hr) (B). (C) Combination of high glucose and low dose H_2O_2 inhibits ERK5 transcriptional activity via p90RSK activation. HUVECs were co-transfected with an empty vector or plasmids encoding DN-p90RSK (lane 21-32), Gal4-ERK5 (lane 1-32), the Gal4-responsive luciferase reporter pG5-luc (lane 1-32), and CA-MEK5α as indicated. Eight hours post transfection, cells were stimulated for 16 hrs by mannitol (25 mM) (lane 3-4, 17-18, 21-22, 25-26, 29-30), H_2O_2 (20 μM) (lane 7-8), D-glucose (25 mM) (lane11-12), a combination of mannitol (25 mM) and H_2O_2 (20 μM) (lane 15-16), or a combination of D-glucose (25 mM) and H_2O_2 (20 μM) (lane 19-20, 23-24, 27-28, 31-32). Then, ERK5 transcriptional activity was assayed as described in Fig.1E. Luciferase activity was normalized relative to Renilla luciferase activity, and expressed as relative fold increase compared with the level of the condition of empty vector transfection for vehicle treatment. Data are representative of three independent experiments (mean ± SEM, n = 3, *p < 0.05, **P < 0.01). (D) HUVECs were pre-treated with

FMK-MEA (10 μM), followed by stimulation with AGE (100 μg/mL) for indicated times. p-p90RSK and p90RSK expression was detected using each specific antibody. (E) HUVECs were co-transfected with plasmids encoding Gal4-ERK5 and the Gal4-responsive luciferase reporter pG5-Luc. Eight hours after transfection, cells were treated with FMK-MEA (10 μM) for 3 hrs, followed by stimulation with 100 μg/mL AGE for 16 hrs. ERK5 transcriptional activity was assayed as described in (C) (mean ± SEM, n = 3, $^{**}P < 0.01$).

Figure S3. p90RSK associates with ERK5 and phosphorylates ERK5-S496.

(A) Association between p90RSK and ERK5 was tested by a mammalian two-hybrid assay. HeLa cells were co-transfected with plasmids encoding Gal4 or Gal4-p90RSK, VP16-ERK5 wild type (see the domain map) or truncated fragments, and the Gal4-responsive luciferase reporter pG5-luc. Luciferase activity was measured after 24 hrs of transfection. Luciferase activity was normalized to the Renilla luciferase activity[28]. Data are representative of three independent experiments (mean ± SEM, n = 3, *P<0.05, $^{**}P < 0.01$). (B, C) H_2O_2 increases ERK5-S496 phosphorylation via p90RSK activation. HUVECs were transduced with either adenovirus vector containing DN-p90RSK or LacZ and 24 hrs later HUVECs were stimulated with H_2O_2 for indicated times. ERK5-S496 phosphorylation, ERK5, p90RSK, and tubulin expression were detected by Western blotting with specific antibodies (B). Phosphorylation level of ERK5-S496 was densitometrically quantified (C) (mean ± SEM, n = 3, *P<0.05).

Figure S4. eNOS, adhesion molecule expressions, p90RSK activation, and apoptosis in non-inducible EC-specific ERK5 knockout mice (ERK5-EKO) and tamoxifen (4-OHT)-treated VE-Cad-CreER^{T2}/WT mice.

(A) TUNEL positive cells (%) in cultured MECs from peanut oil or 4-OHT treated inducible heterozygous ERK5-EKO$^{+/-}$ mice (mean ± SEM, n = 3, N.S.: Not significant). (B) The expressions of ERK5, eNOS, VCAM-1, E-selectin, PECAM-1, p-p90RSK, total p90RSK, cleaved caspase 3, and Tubulin were determined in MECs from non-inducible VE-CadN-wild type (VE-CadN-WT) or homozygous ERK5-EKO$^{-/-}$ (VE-CadN-ERK5$^{flox/flox}$) mice. (C) The expression of ERK5, eNOS, VCAM-1, E-selectin, PECAM-1, p-p90RSK, p90RSK, and Tubulin were determined in MECs from peanut oil or 4-OHT-treated VE-Cad-CreER^{T2}/WT mice. (D) Endothelium-independent relaxation to SNP was measured in 4-OHT-treated VE-Cad-CreER^{T2}/WT or inducible ERK5-EKO$^{-/-}$ mice (mean ± SEM, n = 3, N.S.: Not significant).

Figure S5. Body weight, glucose tolerance test, and plasma cholesterol level in inducible ERK5-EKO$^{-/-}$/LDLR$^{-/-}$ mice.

(A) After 18 weeks of 4-OHT injection and HCD diet, inducible ERK5-EKO$^{-/-}$/LDLR$^{-/-}$ (n = 6) or VE-Cad-CreER^{T2}-WT/LDLR$^{-/-}$ control (n = 6) mice were fasted overnight (16 hours) before the test. Glucose was injected intra-peritoneally (2g/kg) and blood samples were taken before and at 10, 30, 60, and 120 min after the injection of glucose for the measurement of glucose (mean ± SEM). (B) Body weight changes of inducible ERK5-EKO$^{-/-}$/LDLR$^{-/-}$ (n = 6) or VE-Cad-CreER^{T2}-WT/LDLR$^{-/-}$ control (n = 6) mice after 4-OHT treatment. Each mouse at the age of 6-7 weeks was injected with 4-OHT as described in methods. After 2 weeks of 4-OHT treatment body weight was measured at indicated times (mean ± SEM). (C) Cholesterol profiles were from inducible ERK5-EKO$^{-/-}$/LDLR$^{-/-}$ (n = 6) or VE-Cad-CreER^{T2}-WT/LDLR$^{-/-}$ control (n = 8) mice after 18 weeks of 4-OHT injection and HCD diet (mean ± SEM).

Figure S6. FMK-MEA inhibited p90RSK1 and 2 in vivo, but did not have any effect on glucose level, leukocyte count, and EC-independent relaxation in STZ-mediated hyperglycemia.

(A) Chemical structure of FMK-MEA. (B) Bodipy-FMK[29, 30] p90RSK1/2 occupancy assay using heart lysates from mice treated with FMK-MEA. Mice were injected intraperitoneally with FMK-MEA (0, 15, 35 and 50 mg/kg in PBS), and bodipy-FMK p90RSK1/2 occupancy assay was performed as described in the methods. (C-E) FMK-MEA did not have any effect on glucose level, leukocyte count, and EC-independent relaxation in STZ-mediated hyperglycemia. Glucose tests (C) or systemic leukocyte count in the blood (D) in male mice after FMK-MEA or Insulin treatment followed by injection of vehicle or STZ (mean ± SEM, n = 3-4, N.S.: Not significant). STZ injection significantly increased fasting glucose level, whereas FMK-MEA treatment had no effect on STZ-mediated hyperglycemia and systemic leukocyte count. (E) Endothelium-independent relaxation to SNP was measured in C57BL/6 WT mice after injection of vehicle or STZ (mean ± SEM, n = 3, N.S.: Not significant). (F) Cholesterol profiles were from $ApoE^{-/-}$ receiving vehicle, AngII, or AngII + FMK-MEA under normal chow diet for 28 days (mean ± SEM, n = 3-5, N.S.: Not significant).

Supplemental Video Legends

Supplemental Video 1.1-1.2

Leukocyte rolling in micro-vessels of inducibleERK5-EKO mice after peanut oil (1.1) or 4-OHT (1.2) treatment. Intravital microscopy was used to visualize leukocyte rolling in the mesenteric venules.

Supplemental Video 2.1-2.4

Leukocyte rolling in micro-vessels of wild type C57BL/6 mice after vehicle (2.1), STZ alone (2.2), STZ and FMK-MEA (2.3), or STZ and insulin (2.4) treatment. Intravital microscopy was used to visualize leukocyte rolling in the mesenteric venules.

Supplemental Video 3.1-3.3

Leukocyte rolling in micro-vessels of non-transgenic littermate control (NLC) or Akita mice after vehicle (NLC; 3.1, Akita; 3.2) or FMK-MEA (Akita; 3.3) treatment. Intravital microscopy was used to visualize leukocyte rolling in the mesenteric venules.

Supplemental Video 4.1-4.2

Leukocyte rolling in micro-vessels of VE-Cad-CreER^{T2}/WT (4.1) or inducible-EC-WT-p90RSK-Tg mice (4.2). Intravital microscopy was used to visualize leukocyte rolling in the mesenteric venules.

Supplemental Video 5.1-5.5

Leukocyte rolling in micro-vessels of VE-Cad-CreER^{T2}/WT or inducible ERK5-EKO mice after vehicle (VE-Cad-CreER^{T2}/WT; 5.1, inducible ERK5-EKO; 5.2), STZ alone (inducible ERK5-EKO; 5.3), FMK-MEA alone (inducible ERK5-EKO; 5.4) or STZ and FMK-MEA (inducible ERK5-EKO; 5.5) treatment. Intravital microscopy was used to visualize leukocyte rolling in the mesenteric venules.

Supplemental References

1. Monvoisin A, Alva JA, Hofmann JJ, Zovein AC, Lane TF, Iruela-Arispe ML. Ve-cadherin-creert2 transgenic mouse: A model for inducible recombination in the endothelium. *Dev Dyn*. 2006;235:3413-3422

2. Kimura TE, Jin J, Zi M, Prehar S, Liu W, Oceandy D, Abe J, Neyses L, Weston AH, Cartwright EJ, Wang X. Targeted deletion of the extracellular signal-regulated protein kinase 5 attenuates hypertrophic response and promotes pressure overload-induced apoptosis in the heart. *Circ Res*. 2010;106:961-970

3. Novak A, Guo C, Yang W, Nagy A, Lobe CG. Z/eg, a double reporter mouse line that expresses enhanced green fluorescent protein upon cre-mediated excision. *Genesis*. 2000;28:147-155

4. C.F. Barbas r, Burton DR, Scott JK, Silverman GJ. *Phage display: A laboratory manual*. 2011.

5. Haidaris CG, Malone J, Sherrill LA, Bliss JM, Gaspari AA, Insel RA, Sullivan MA. Recombinant human antibody single chain variable fragments reactive with candida albicans surface antigens. *J Immunol Methods*. 2001;257:185-202

6. Shea C, Bloedorn L, Sullivan MA. Rapid isolation of single-chain antibodies for structural genomics. *J Struct Funct Genomics*. 2005;6:171-175

7. Tiller T, Meffre E, Yurasov S, Tsuiji M, Nussenzweig MC, Wardemann H. Efficient generation of monoclonal antibodies from single human b cells by single cell rt-pcr and expression vector cloning. *J Immunol Methods*. 2008;329:112-124

8. Maekawa N, Abe J, Shishido T, Itoh S, Ding B, Sharma VK, Sheu SS, Blaxall BC, Berk BC. Inhibiting p90 ribosomal s6 kinase prevents (na+)-h+ exchanger-mediated cardiac ischemia-reperfusion injury. *Circulation*. 2006;113:2516-2523

9. Cameron SJ, Malik S, Akaike M, Lerner-Marmarosh N, Yan C, Lee JD, Abe J, Yang J. Regulation of epidermal growth factor-induced connexin 43 gap junction communication by big mitogen-activated protein kinase1/erk5 but not erk1/2 kinase activation. *J Biol Chem*. 2003;278:18682-18688

10. Takahashi M, Berk BC. Mitogen-activated protein kinase (erk1/2) activation by shear stress and adhesion in endothelial cells. Essential role for a herbimycin-sensitive kinase. *J Clin Invest*. 1996;98:2623-2631

11. Pi X, Yan C, Berk BC. Big mitogen-activated protein kinase (bmk1)/erk5 protects endothelial cells from apoptosis. *Circ Res*. 2004;94:362-369

12. Daugherty A, Manning MW, Cassis LA. Angiotensin ii promotes atherosclerotic lesions and aneurysms in apolipoprotein e-deficient mice. *J Clin Invest*. 2000;105:1605-1612.

13. Lim YC, Luscinskas FW. Isolation and culture of murine heart and lung endothelial cells for in vitro model systems. *Methods Mol Biol*. 2006;341:141-154

14. Hosking BM, Wang SC, Downes M, Koopman P, Muscat GE. The vcam-1 gene that encodes the vascular cell adhesion molecule is a target of the sry-related high mobility group box gene, sox18. *J Biol Chem*. 2004;279:5314-5322

15. Adluri RS, Thirunavukkarasu M, Dunna NR, Zhan L, Oriowo B, Takeda K, Sanchez JA, Otani H, Maulik G, Fong GH, Maulik N. Disruption of hypoxia-inducible transcription factor-prolyl hydroxylase domain-1 (phd-1-/-) attenuates ex vivo myocardial ischemia/reperfusion

injury through hypoxia-inducible factor-1alpha transcription factor and its target genes in mice. *Antioxid Redox Signal*. 2011;15:1789-1797

16. Bro S, Moeller F, Andersen CB, Olgaard K, Nielsen LB. Increased expression of adhesion molecules in uremic atherosclerosis in apolipoprotein-e-deficient mice. *J Am Soc Nephrol*. 2004;15:1495-1503

17. Abe J, Takahashi M, Ishida M, Lee JD, Berk BC. C-src is required for oxidative stress-mediated activation of big mitogen-activated protein kinase 1. *J Biol Chem*. 1997;272:20389-20394

18. Akaike M, Che W, Marmarosh NL, Ohta S, Osawa M, Ding B, Berk BC, Yan C, Abe J. The hinge-helix 1 region of peroxisome proliferator-activated receptor gamma1 (ppargamma1) mediates interaction with extracellular signal-regulated kinase 5 and ppargamma1 transcriptional activation: Involvement in flow-induced ppargamma activation in endothelial cells. *Mol Cell Biol*. 2004;24:8691-8704

19. Hajra L, Evans AI, Chen M, Hyduk SJ, Collins T, Cybulsky MI. The nf-kappa b signal transduction pathway in aortic endothelial cells is primed for activation in regions predisposed to atherosclerotic lesion formation. *Proc Natl Acad Sci U S A*. 2000;97:9052-9057.

20. Iiyama K, Hajra L, Iiyama M, Li H, DiChiara M, Medoff BD, Cybulsky MI. Patterns of vascular cell adhesion molecule-1 and intercellular adhesion molecule-1 expression in rabbit and mouse atherosclerotic lesions and at sites predisposed to lesion formation. *Circ Res*. 1999;85:199-207.

21. Cambien B, Bergmeier W, Saffaripour S, Mitchell HA, Wagner DD. Antithrombotic activity of tnf-alpha. *J Clin Invest*. 2003;112:1589-1596

22. Piqueras L, Sanz MJ, Perretti M, Morcillo E, Norling L, Mitchell JA, Li Y, Bishop-Bailey D. Activation of pparbeta/delta inhibits leukocyte recruitment, cell adhesion molecule expression, and chemokine release. *J Leukoc Biol*. 2009;86:115-122

23. Morrell CN, Matsushita K, Lowenstein CJ. A novel inhibitor of n-ethylmaleimide-sensitive factor decreases leukocyte trafficking and peritonitis. *J Pharmacol Exp Ther*. 2005;314:155-161

24. Karaman MW, Herrgard S, Treiber DK, Gallant P, Atteridge CE, Campbell BT, Chan KW, Ciceri P, Davis MI, Edeen PT, Faraoni R, Floyd M, Hunt JP, Lockhart DJ, Milanov ZV, Morrison MJ, Pallares G, Patel HK, Pritchard S, Wodicka LM, Zarrinkar PP. A quantitative analysis of kinase inhibitor selectivity. *Nat Biotechnol*. 2008;26:127-132

25. Fabian MA, Biggs WH, 3rd, Treiber DK, Atteridge CE, Azimioara MD, Benedetti MG, Carter TA, Ciceri P, Edeen PT, Floyd M, Ford JM, Galvin M, Gerlach JL, Grotzfeld RM, Herrgard S, Insko DE, Insko MA, Lai AG, Lelias JM, Mehta SA, Milanov ZV, Velasco AM, Wodicka LM, Patel HK, Zarrinkar PP, Lockhart DJ. A small molecule-kinase interaction map for clinical kinase inhibitors. *Nat Biotechnol*. 2005;23:329-336

26. Fernandez-Hernando C, Ackah E, Yu J, Suarez Y, Murata T, Iwakiri Y, Prendergast J, Miao RQ, Birnbaum MJ, Sessa WC. Loss of akt1 leads to severe atherosclerosis and occlusive coronary artery disease. *Cell Metab*. 2007;6:446-457

27. Patricelli MP, Nomanbhoy TK, Wu J, Brown H, Zhou D, Zhang J, Jagannathan S, Aban A, Okerberg E, Herring C, Nordin B, Weissig H, Yang Q, Lee JD, Gray NS, Kozarich JW. In situ kinase profiling reveals functionally relevant properties of native kinases. *Chem Biol*. 2011;18:699-710

28. Woo CH, Shishido T, McClain C, Lim JH, Li JD, Yang J, Yan C, Abe J. Extracellular signal-regulated kinase 5 sumoylation antagonizes shear stress-induced antiinflammatory response and endothelial nitric oxide synthase expression in endothelial cells. *Circ Res*. 2008;102:538-545

29. Serafimova IM, Pufall MA, Krishnan S, Duda K, Cohen MS, Maglathlin RL, McFarland JM, Miller RM, Frodin M, Taunton J. Reversible targeting of noncatalytic cysteines with chemically tuned electrophiles. *Nat Chem Biol*. 2012;8:471-476

30. Cohen MS, Hadjivassiliou H, Taunton J. A clickable inhibitor reveals context-dependent autoactivation of p90 rsk. *Nat Chem Biol*. 2007;3:156-160

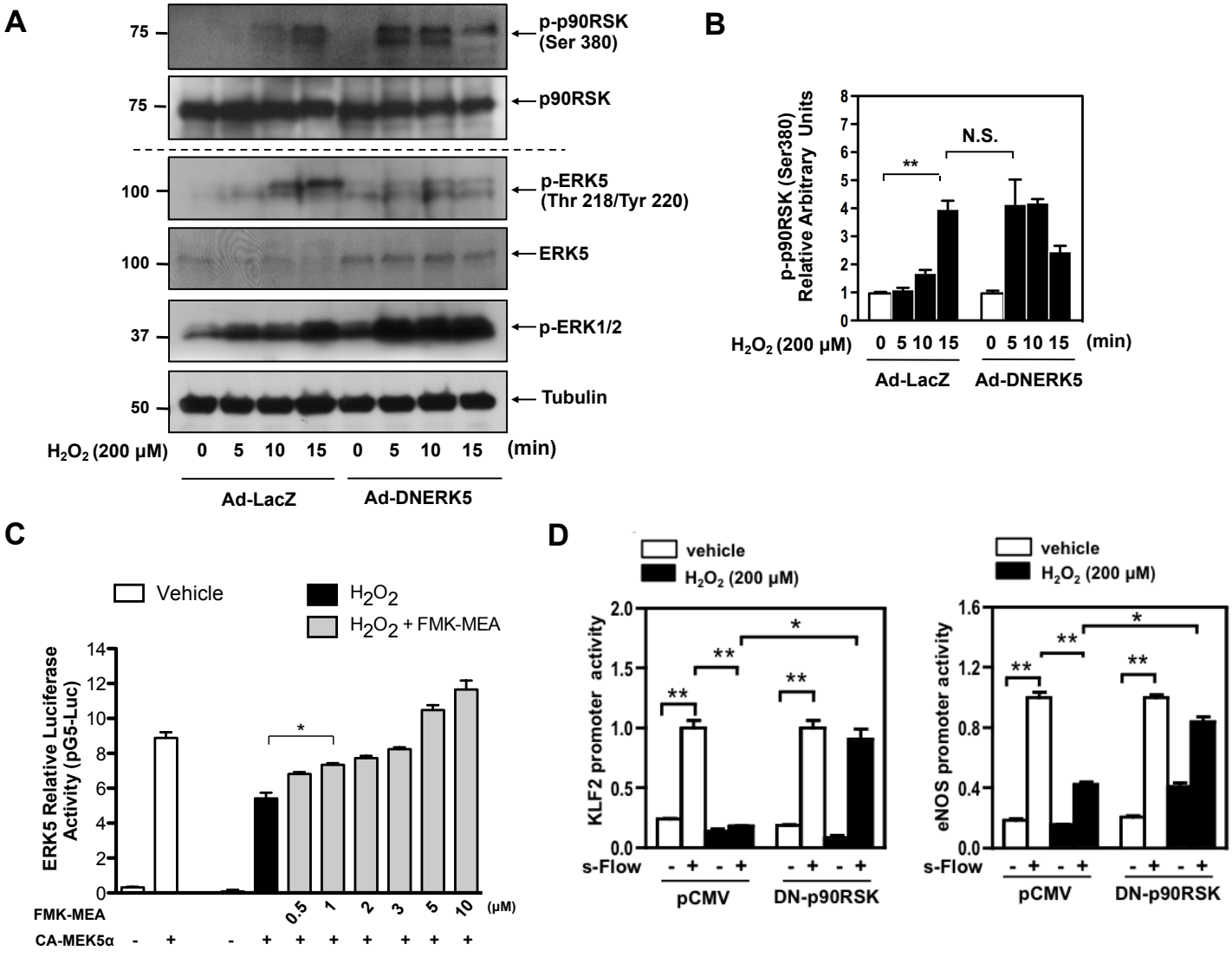
A
75
p-p90RSK (Ser 380)
75
p90RSK
100
p-ERK5 (Thr 218/Tyr 220)
100
ERK5
37
p-ERK1/2
50
Tubulin
H2O2 (200 μM) 0 5 10 15 0 5 10 15 (min)
Ad-LacZ
Ad-DNERK5
B
p-p90RSK (Ser380) Relative Arbitrary Units
N.S.
**
H2O2 (200 μM) 0 5 10 15 0 5 10 15 (min)
Ad-LacZ
Ad-DNERK5
C
Vehicle
H2O2
H2O2 + FMK-MEA
ERK5 Relative Luciferase Activity (pG5-Luc)
*
FMK-MEA 0.5 1 2 3 5 10 (μM)
CA-MEK5α - + - + + + + + + +
D
vehicle
H2O2 (200 μM)
KLF2 promoter activity
s-Flow - + - + - + - +
pCMV
DN-p90RSK
eNOS promoter activity

Fig. S1

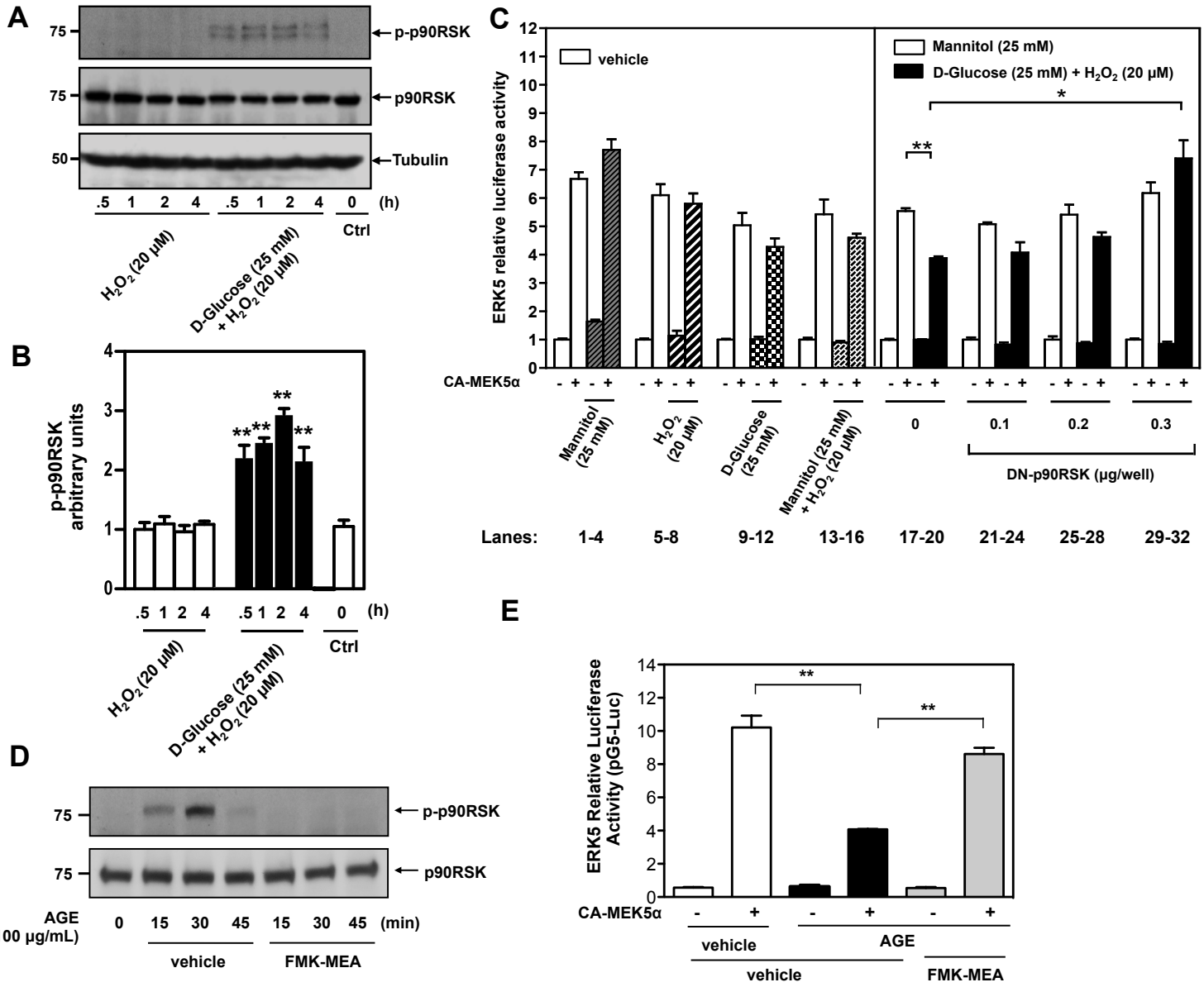
A
75
p-p90RSK
75
p90RSK
50
Tubulin
.5 1 2 4 .5 1 2 4 0 (h)
H2O2 (20 μM)
D-Glucose (25 mM) + H2O2 (20 μM)
Ctrl
B
p-p90RSK arbitrary units
.5 1 2 4 .5 1 2 4 0 (h)
H2O2 (20 μM)
D-Glucose (25 mM) + H2O2 (20 μM)
Ctrl
C
ERK5 relative luciferase activity
vehicle
Mannitol (25 mM)
D-Glucose (25 mM) + H2O2 (20 μM)
CA-MEK5α
Mannitol (25 mM)
H2O2 (20 μM)
D-Glucose (25 mM)
Mannitol (25 mM) + H2O2 (20 μM)
0
0.1
0.2
0.3
DN-p90RSK (μg/well)
Lanes: 1-4 5-8 9-12 13-16 17-20 21-24 25-28 29-32
D
75
p-p90RSK
75
p90RSK
AGE (100 μg/mL)
0 15 30 45 15 30 45 (min)
vehicle
FMK-MEA
E
ERK5 Relative Luciferase Activity (pG5-Luc)
CA-MEK5α
vehicle
AGE
vehicle
FMK-MEA

Fig. S2

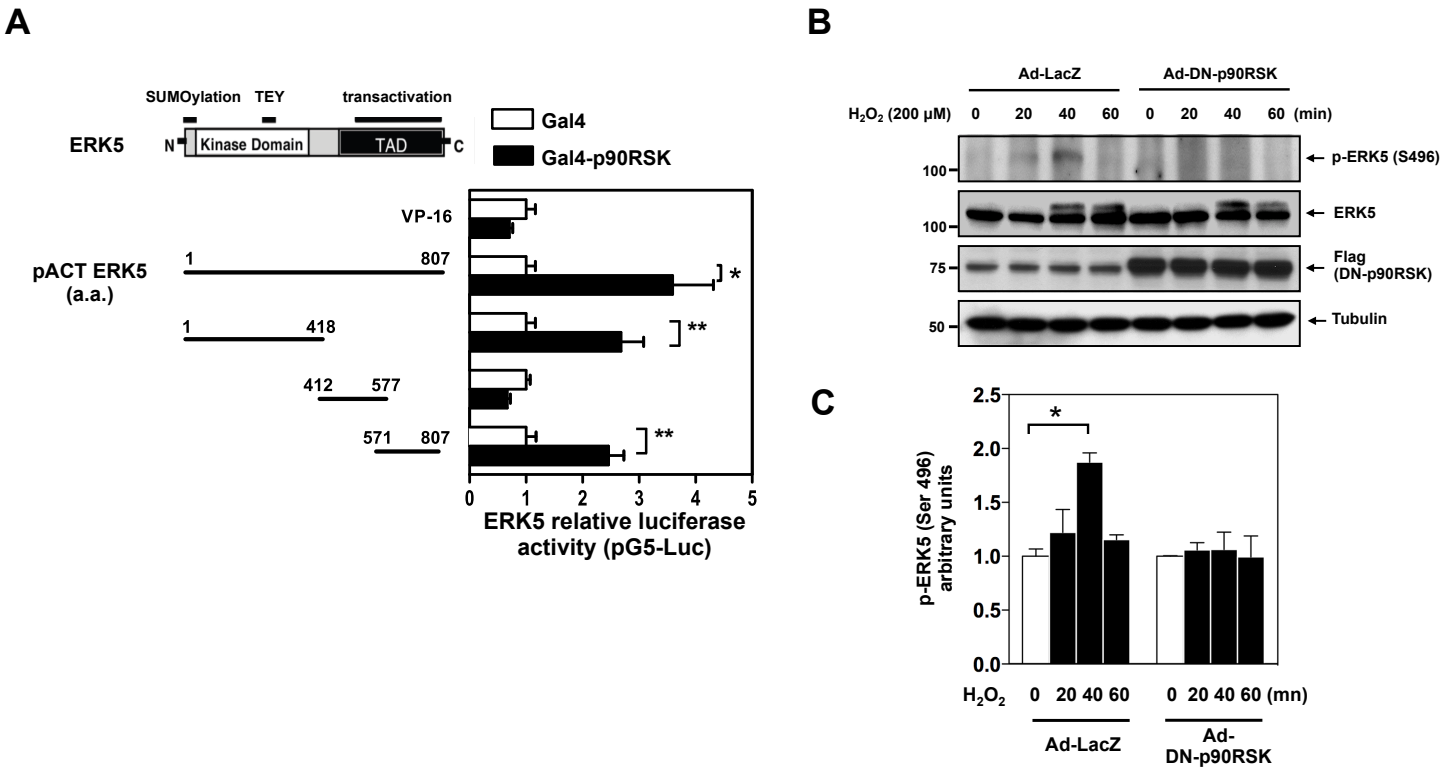
A
SUMOylation
TEY
transactivation
ERK5
N
Kinase Domain
TAD
C
Gal4
Gal4-p90RSK
VP-16
pACT ERK5
(a.a.)
1
807
1
418
412
577
571
807
*
**
**
0
1
2
3
4
5
ERK5 relative luciferase
activity (pG5-Luc)
B
Ad-LacZ
Ad-DN-p90RSK
H2O2 (200 μM)
0
20
40
60
0
20
40
60
(min)
100
100
75
50
p-ERK5 (S496)
ERK5
Flag
(DN-p90RSK)
Tubulin
C
p-ERK5 (Ser 496)
arbitrary units
2.5
2.0
1.5
1.0
0.5
0.0
*
H2O2
0
20
40
60
0
20
40
60
(mn)
Ad-LacZ
Ad-
DN-p90RSK

Fig. S3

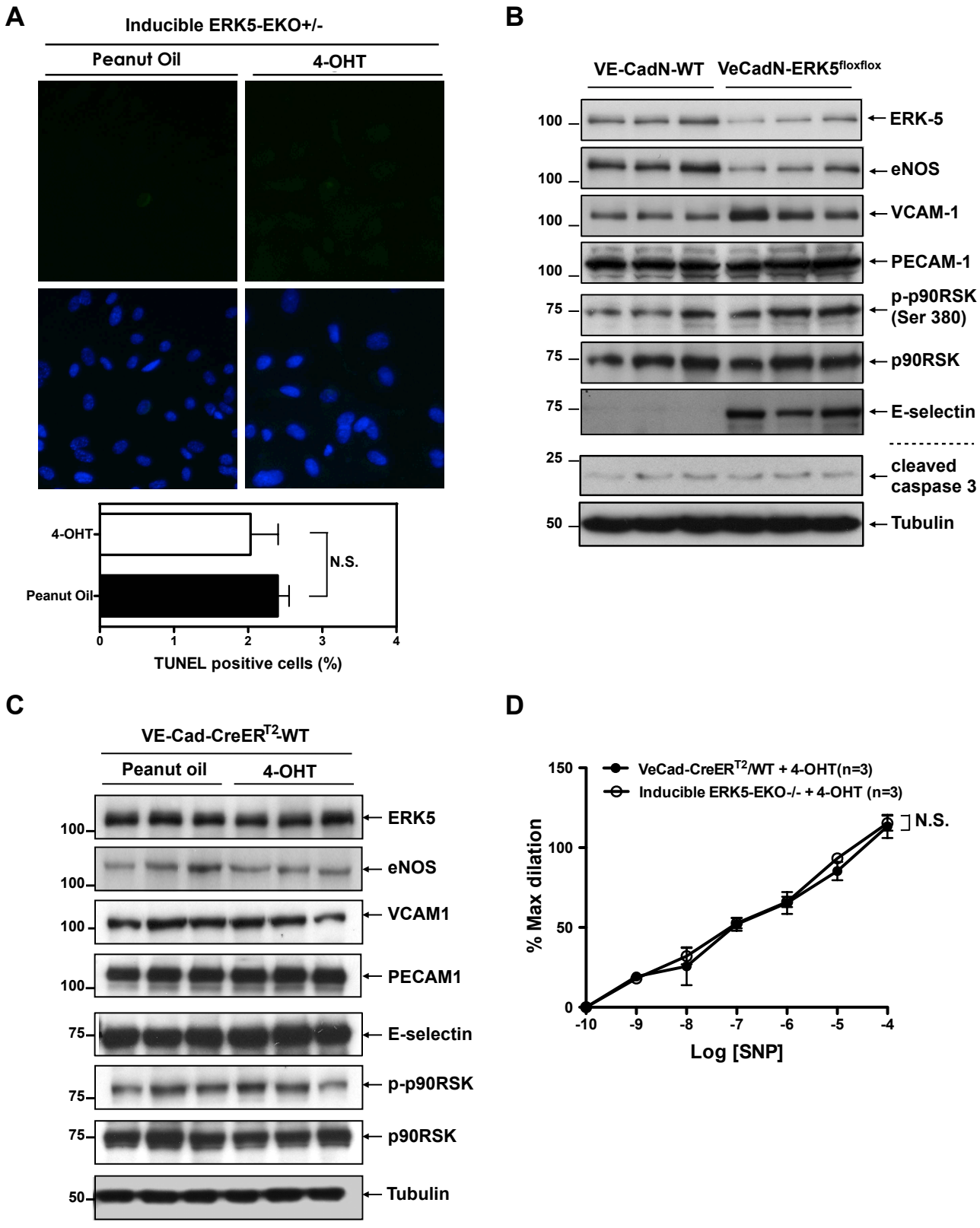
A
Inducible ERK5-EKO+/-
Peanut Oil
4-OHT
4-OHT
Peanut Oil
N.S.
0
1
2
3
4
TUNEL positive cells (%)
B
VE-CadN-WT
VeCadN-ERK5floxflox
100
ERK-5
100
eNOS
100
VCAM-1
100
PECAM-1
75
p-p90RSK (Ser 380)
75
p90RSK
75
E-selectin
25
cleaved caspase 3
50
Tubulin
C
VE-Cad-CreER^{T2}-WT
Peanut oil
4-OHT
100
ERK5
100
eNOS
100
VCAM1
100
PECAM1
75
E-selectin
75
p-p90RSK
75
p90RSK
50
Tubulin
D
VeCad-CreER^{T2}/WT + 4-OHT(n=3)
Inducible ERK5-EKO-/- + 4-OHT (n=3)
N.S.
% Max dilation
150
100
50
0
-10
-9
-8
-7
-6
-5
-4
Log [SNP]

Fig. S4

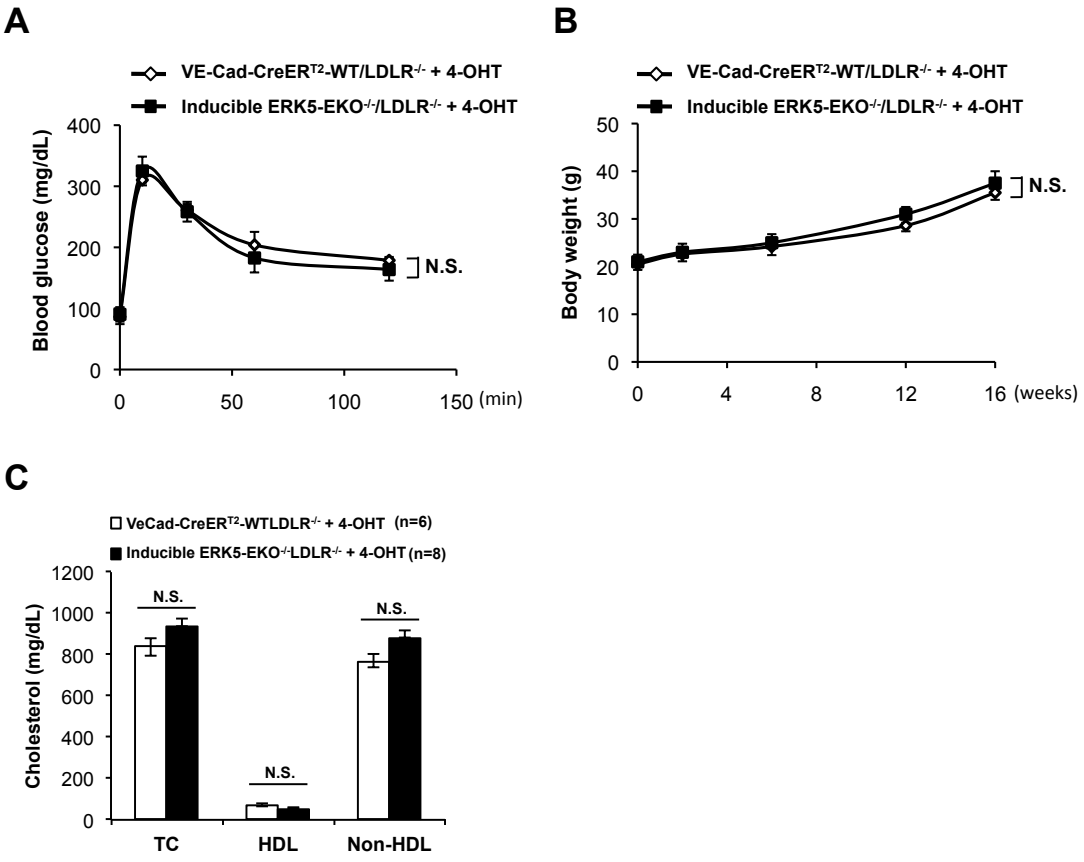
A
VE-Cad-CreER^{T2}-WT/LDLR$^{-/-}$ + 4-OHT
Inducible ERK5-EKO$^{-/-}$/LDLR$^{-/-}$ + 4-OHT
Blood glucose (mg/dL)
400
300
200
100
0
0
50
100
150 (min)
N.S.
B
VE-Cad-CreER^{T2}-WT/LDLR$^{-/-}$ + 4-OHT
Inducible ERK5-EKO$^{-/-}$/LDLR$^{-/-}$ + 4-OHT
Body weight (g)
50
40
30
20
10
0
0
4
8
12
16 (weeks)
N.S.
C
VeCad-CreER^{T2}-WTLDLR$^{-/-}$ + 4-OHT (n=6)
Inducible ERK5-EKO$^{-/-}$LDLR$^{-/-}$ + 4-OHT (n=8)
Cholesterol (mg/dL)
1200
1000
800
600
400
200
0
N.S.
N.S.
N.S.
TC
HDL
Non-HDL

Fig. S5

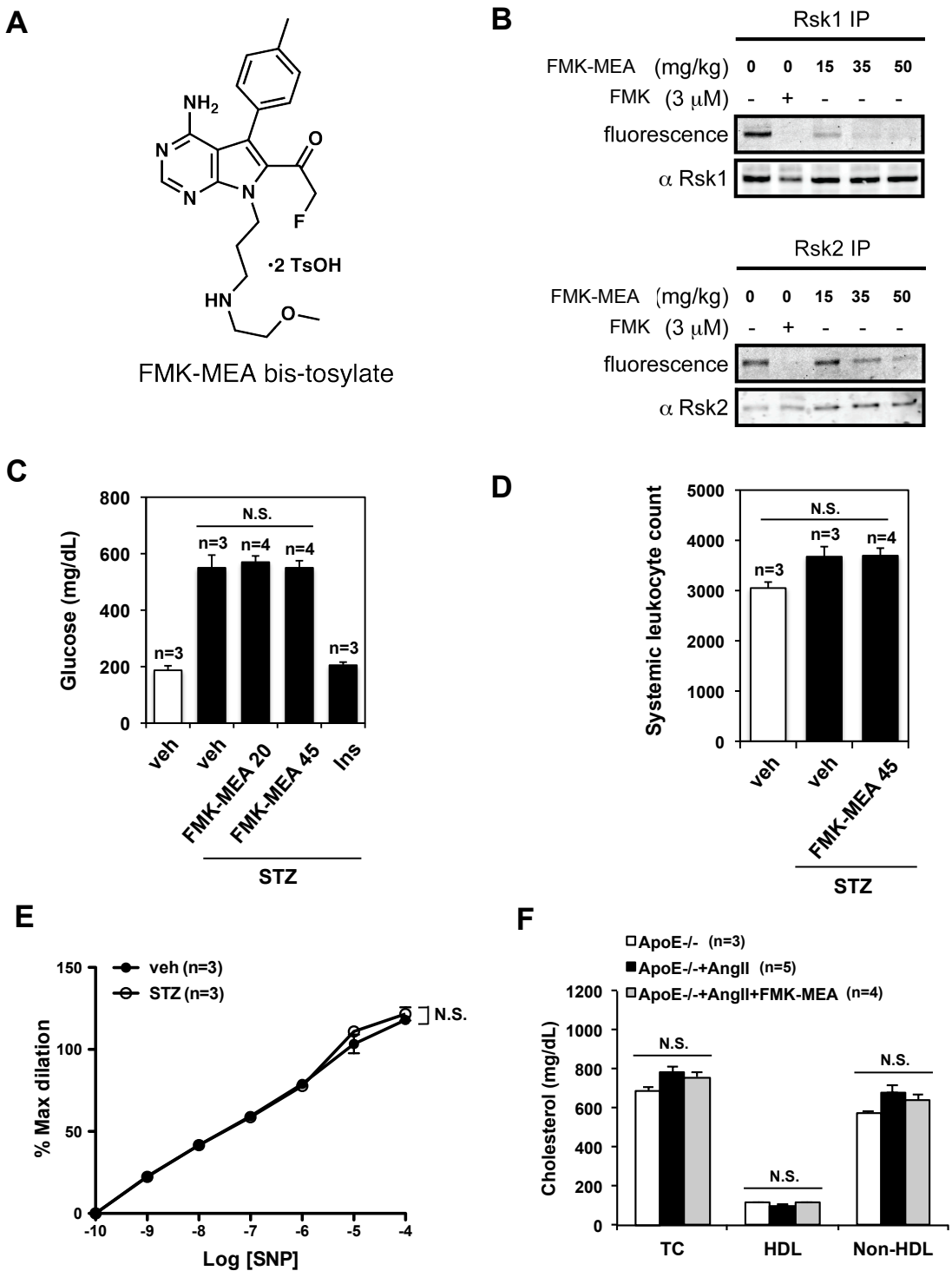
A
NH2
N
N
N
O
F
·2 TsOH
HN
O
FMK-MEA bis-tosylate
B
Rsk1 IP
FMK-MEA (mg/kg) 0 0 15 35 50
FMK (3 μM) - + - - -
fluorescence
α Rsk1
Rsk2 IP
FMK-MEA (mg/kg) 0 0 15 35 50
FMK (3 μM) - + - - -
fluorescence
α Rsk2
C
Glucose (mg/dL)
800
600
400
200
0
N.S.
n=3
n=4
n=4
n=3
n=3
veh
veh
FMK-MEA 20
FMK-MEA 45
Ins
STZ
D
Systemic leukocyte count
5000
4000
3000
2000
1000
0
N.S.
n=3
n=3
n=4
veh
veh
FMK-MEA 45
STZ
E
% Max dilation
150
100
50
0
veh (n=3)
STZ (n=3)
N.S.
-10
-9
-8
-7
-6
-5
-4
Log [SNP]
F
ApoE-/- (n=3)
ApoE-/-+AngII (n=5)
ApoE-/-+AngII+FMK-MEA (n=4)
Cholesterol (mg/dL)
1200
1000
800
600
400
200
0
N.S.
N.S.
N.S.
TC
HDL
Non-HDL

Fig. S6

Table S1. Ambit/DiscoverX platform secreening

Compound Name	Ambit Gene Symbol	Entrez Gene Symbol	Percent Control	Compound Concentration (nM)
FMK-MEA	AAK1	AAK1	95	1000
FMK-MEA	ABL1(E255K)-phosphorylated	ABL1	90	1000
FMK-MEA	ABL1(F317I)-nonphosphorylated	ABL1	71	1000
FMK-MEA	ABL1(F317I)-phosphorylated	ABL1	72	1000
FMK-MEA	ABL1(F317L)-nonphosphorylated	ABL1	82	1000
FMK-MEA	ABL1(F317L)-phosphorylated	ABL1	81	1000
FMK-MEA	ABL1(H396P)-nonphosphorylated	ABL1	87	1000
FMK-MEA	ABL1(H396P)-phosphorylated	ABL1	86	1000
FMK-MEA	ABL1(M351T)-phosphorylated	ABL1	96	1000
FMK-MEA	ABL1(Q252H)-nonphosphorylated	ABL1	93	1000
FMK-MEA	ABL1(Q252H)-phosphorylated	ABL1	95	1000
FMK-MEA	ABL1(T315I)-nonphosphorylated	ABL1	100	1000
FMK-MEA	ABL1(T315I)-phosphorylated	ABL1	100	1000
FMK-MEA	ABL1(Y253F)-phosphorylated	ABL1	94	1000
FMK-MEA	ABL1-nonphosphorylated	ABL1	98	1000
FMK-MEA	ABL1-phosphorylated	ABL1	83	1000
FMK-MEA	ABL2	ABL2	100	1000
FMK-MEA	ACVR1	ACVR1	100	1000
FMK-MEA	ACVR1B	ACVR1B	91	1000
FMK-MEA	ACVR2A	ACVR2A	100	1000
FMK-MEA	ACVR2B	ACVR2B	95	1000
FMK-MEA	ACVRL1	ACVRL1	100	1000
FMK-MEA	ADCK3	CABC1	100	1000
FMK-MEA	ADCK4	ADCK4	93	1000
FMK-MEA	AKT1	AKT1	100	1000
FMK-MEA	AKT2	AKT2	95	1000
FMK-MEA	AKT3	AKT3	86	1000
FMK-MEA	ALK	ALK	71	1000
FMK-MEA	AMPK-alpha1	PRKAA1	100	1000
FMK-MEA	AMPK-alpha2	PRKAA2	75	1000
FMK-MEA	ANKK1	ANKK1	100	1000
FMK-MEA	ARK5	NUAK1	98	1000
FMK-MEA	ASK1	MAP3K5	100	1000
FMK-MEA	ASK2	MAP3K6	100	1000
FMK-MEA	AURKA	AURKA	92	1000
FMK-MEA	AURKB	AURKB	62	1000
FMK-MEA	AURKC	AURKC	89	1000
FMK-MEA	AXL	AXL	81	1000
FMK-MEA	BIKE	BMP2K	94	1000
FMK-MEA	BLK	BLK	100	1000
FMK-MEA	BMPR1A	BMPR1A	100	1000
FMK-MEA	BMPR1B	BMPR1B	85	1000
FMK-MEA	BMPR2	BMPR2	72	1000
FMK-MEA	BMX	BMX	98	1000
FMK-MEA	BRAF	BRAF	72	1000
FMK-MEA	BRAF(V600E)	BRAF	74	1000
FMK-MEA	BRK	PTK6	90	1000
FMK-MEA	BRSK1	BRSK1	82	1000
FMK-MEA	BRSK2	BRSK2	100	1000
FMK-MEA	BTK	BTK	87	1000
FMK-MEA	CAMK1	CAMK1	100	1000
FMK-MEA	CAMK1D	CAMK1D	100	1000
FMK-MEA	CAMK1G	CAMK1G	97	1000
FMK-MEA	CAMK2A	CAMK2A	78	1000
FMK-MEA	CAMK2B	CAMK2B	97	1000
FMK-MEA	CAMK2D	CAMK2D	82	1000
FMK-MEA	CAMK2G	CAMK2G	100	1000
FMK-MEA	CAMK4	CAMK4	100	1000
FMK-MEA	CAMKK1	CAMKK1	100	1000
FMK-MEA	CAMKK2	CAMKK2	100	1000
FMK-MEA	CASK	CASK	62	1000
FMK-MEA	CDC2L1	CDC2L1	100	1000
FMK-MEA	CDC2L2	CDC2L2	100	1000
FMK-MEA	CDC2L5	CDC2L5	90	1000
FMK-MEA	CDK11	CDC2L6	98	1000

FMK-MEA	CDK2	CDK2	83	1000
FMK-MEA	CDK3	CDK3	100	1000
FMK-MEA	CDK4-cyclinD1	CDK4	98	1000
FMK-MEA	CDK4-cyclinD3	CDK4	100	1000
FMK-MEA	CDK5	CDK5	95	1000
FMK-MEA	CDK7	CDK7	100	1000
FMK-MEA	CDK8	CDK8	100	1000
FMK-MEA	CDK9	CDK9	100	1000
FMK-MEA	CDKL1	CDKL1	100	1000
FMK-MEA	CDKL2	CDKL2	87	1000
FMK-MEA	CDKL3	CDKL3	88	1000
FMK-MEA	CDKL5	CDKL5	100	1000
FMK-MEA	CHEK1	CHEK1	100	1000
FMK-MEA	CHEK2	CHEK2	100	1000
FMK-MEA	CIT	CIT	93	1000
FMK-MEA	CLK1	CLK1	87	1000
FMK-MEA	CLK2	CLK2	100	1000
FMK-MEA	CLK3	CLK3	79	1000
FMK-MEA	CLK4	CLK4	91	1000
FMK-MEA	CSF1R	CSF1R	89	1000
FMK-MEA	CSK	CSK	95	1000
FMK-MEA	CSNK1A1	CSNK1A1	100	1000
FMK-MEA	CSNK1A1L	CSNK1A1L	100	1000
FMK-MEA	CSNK1D	CSNK1D	82	1000
FMK-MEA	CSNK1E	CSNK1E	87	1000
FMK-MEA	CSNK1G1	CSNK1G1	91	1000
FMK-MEA	CSNK1G2	CSNK1G2	100	1000
FMK-MEA	CSNK1G3	CSNK1G3	98	1000
FMK-MEA	CSNK2A1	CSNK2A1	100	1000
FMK-MEA	CSNK2A2	CSNK2A2	99	1000
FMK-MEA	CTK	MATK	100	1000
FMK-MEA	DAPK1	DAPK1	100	1000
FMK-MEA	DAPK2	DAPK2	97	1000
FMK-MEA	DAPK3	DAPK3	97	1000
FMK-MEA	DCAMKL1	DCLK1	100	1000
FMK-MEA	DCAMKL2	DCLK2	100	1000
FMK-MEA	DCAMKL3	DCLK3	100	1000
FMK-MEA	DDR1	DDR1	100	1000
FMK-MEA	DDR2	DDR2	99	1000
FMK-MEA	DLK	MAP3K12	94	1000
FMK-MEA	DMPK	DMPK	84	1000
FMK-MEA	DMPK2	CDC42BPG	84	1000
FMK-MEA	DRAK1	STK17A	98	1000
FMK-MEA	DRAK2	STK17B	96	1000
FMK-MEA	DYRK1A	DYRK1A	100	1000
FMK-MEA	DYRK1B	DYRK1B	96	1000
FMK-MEA	DYRK2	DYRK2	89	1000
FMK-MEA	EGFR	EGFR	96	1000
FMK-MEA	EGFR(E746-A750del)	EGFR	100	1000
FMK-MEA	EGFR(G719C)	EGFR	84	1000
FMK-MEA	EGFR(G719S)	EGFR	90	1000
FMK-MEA	EGFR(L747-E749del, A750P)	EGFR	67	1000
FMK-MEA	EGFR(L747-S752del, P753S)	EGFR	100	1000
FMK-MEA	EGFR(L747-T751del,Sins)	EGFR	84	1000
FMK-MEA	EGFR(L858R)	EGFR	62	1000
FMK-MEA	EGFR(L858R,T790M)	EGFR	100	1000
FMK-MEA	EGFR(L861Q)	EGFR	84	1000
FMK-MEA	EGFR(S752-I759del)	EGFR	90	1000
FMK-MEA	EGFR(T790M)	EGFR	100	1000
FMK-MEA	EIF2AK1	EIF2AK1	100	1000
FMK-MEA	EPHA1	EPHA1	94	1000
FMK-MEA	EPHA2	EPHA2	100	1000
FMK-MEA	EPHA3	EPHA3	88	1000
FMK-MEA	EPHA4	EPHA4	96	1000
FMK-MEA	EPHA5	EPHA5	91	1000
FMK-MEA	EPHA6	EPHA6	82	1000

FMK-MEA	EPHA7	EPHA7	92	1000
FMK-MEA	EPHA8	EPHA8	75	1000
FMK-MEA	EPHB1	EPHB1	94	1000
FMK-MEA	EPHB2	EPHB2	92	1000
FMK-MEA	EPHB3	EPHB3	100	1000
FMK-MEA	EPHB4	EPHB4	89	1000
FMK-MEA	EPHB6	EPHB6	100	1000
FMK-MEA	ERBB2	ERBB2	100	1000
FMK-MEA	ERBB3	ERBB3	96	1000
FMK-MEA	ERBB4	ERBB4	100	1000
FMK-MEA	ERK1	MAPK3	98	1000
FMK-MEA	ERK2	MAPK1	100	1000
FMK-MEA	ERK3	MAPK6	100	1000
FMK-MEA	ERK4	MAPK4	100	1000
FMK-MEA	ERK5	MAPK7	100	1000
FMK-MEA	ERK8	MAPK15	96	1000
FMK-MEA	ERN1	ERN1	99	1000
FMK-MEA	FAK	PTK2	100	1000
FMK-MEA	FER	FER	84	1000
FMK-MEA	FES	FES	100	1000
FMK-MEA	FGFR1	FGFR1	98	1000
FMK-MEA	FGFR2	FGFR2	100	1000
FMK-MEA	FGFR3	FGFR3	92	1000
FMK-MEA	FGFR3(G697C)	FGFR3	91	1000
FMK-MEA	FGFR4	FGFR4	100	1000
FMK-MEA	FGR	FGR	93	1000
FMK-MEA	FLT1	FLT1	96	1000
FMK-MEA	FLT3	FLT3	71	1000
FMK-MEA	FLT3(D835H)	FLT3	100	1000
FMK-MEA	FLT3(D835Y)	FLT3	100	1000
FMK-MEA	FLT3(ITD)	FLT3	91	1000
FMK-MEA	FLT3(K663Q)	FLT3	100	1000
FMK-MEA	FLT3(N841I)	FLT3	65	1000
FMK-MEA	FLT3(R834Q)	FLT3	96	1000
FMK-MEA	FLT4	FLT4	98	1000
FMK-MEA	FRK	FRK	81	1000
FMK-MEA	FYN	FYN	87	1000
FMK-MEA	GAK	GAK	100	1000
FMK-MEA	GCN2(Kin.Dom.2,S808G)	EIF2AK4	100	1000
FMK-MEA	GRK1	GRK1	100	1000
FMK-MEA	GRK4	GRK4	85	1000
FMK-MEA	GRK7	GRK7	100	1000
FMK-MEA	GSK3A	GSK3A	100	1000
FMK-MEA	GSK3B	GSK3B	100	1000
FMK-MEA	HCK	HCK	100	1000
FMK-MEA	HIPK1	HIPK1	96	1000
FMK-MEA	HIPK2	HIPK2	94	1000
FMK-MEA	HIPK3	HIPK3	100	1000
FMK-MEA	HIPK4	HIPK4	95	1000
FMK-MEA	HPK1	MAP4K1	86	1000
FMK-MEA	HUNK	HUNK	100	1000
FMK-MEA	ICK	ICK	100	1000
FMK-MEA	IGF1R	IGF1R	100	1000
FMK-MEA	IKK-alpha	CHUK	72	1000
FMK-MEA	IKK-beta	IKBKB	95	1000
FMK-MEA	IKK-epsilon	IKBKE	100	1000
FMK-MEA	INSR	INSR	84	1000
FMK-MEA	INSRR	INSRR	100	1000
FMK-MEA	IRAK1	IRAK1	93	1000
FMK-MEA	IRAK3	IRAK3	86	1000
FMK-MEA	IRAK4	IRAK4	100	1000
FMK-MEA	ITK	ITK	100	1000
FMK-MEA	JAK1(JH1domain-catalytic)	JAK1	100	1000
FMK-MEA	JAK1(JH2domain-pseudokinase)	JAK1	100	1000
FMK-MEA	JAK2(JH1domain-catalytic)	JAK2	100	1000
FMK-MEA	JAK3(JH1domain-catalytic)	JAK3	100	1000

FMK-MEA	JNK1	MAPK8	96	1000
FMK-MEA	JNK2	MAPK9	94	1000
FMK-MEA	JNK3	MAPK10	100	1000
FMK-MEA	KIT	KIT	77	1000
FMK-MEA	KIT(A829P)	KIT	85	1000
FMK-MEA	KIT(D816H)	KIT	97	1000
FMK-MEA	KIT(D816V)	KIT	96	1000
FMK-MEA	KIT(L576P)	KIT	71	1000
FMK-MEA	KIT(V559D)	KIT	73	1000
FMK-MEA	KIT(V559D,T670I)	KIT	86	1000
FMK-MEA	KIT(V559D,V654A)	KIT	94	1000
FMK-MEA	LATS1	LATS1	100	1000
FMK-MEA	LATS2	LATS2	100	1000
FMK-MEA	LCK	LCK	65	1000
FMK-MEA	LIMK1	LIMK1	100	1000
FMK-MEA	LIMK2	LIMK2	100	1000
FMK-MEA	LKB1	STK11	98	1000
FMK-MEA	LOK	STK10	100	1000
FMK-MEA	LRRK2	LRRK2	100	1000
FMK-MEA	LRRK2(G2019S)	LRRK2	100	1000
FMK-MEA	LTK	LTK	100	1000
FMK-MEA	LYN	LYN	97	1000
FMK-MEA	LZK	MAP3K13	92	1000
FMK-MEA	MAK	MAK	95	1000
FMK-MEA	MAP3K1	MAP3K1	100	1000
FMK-MEA	MAP3K15	MAP3K15	100	1000
FMK-MEA	MAP3K2	MAP3K2	90	1000
FMK-MEA	MAP3K3	MAP3K3	96	1000
FMK-MEA	MAP3K4	MAP3K4	100	1000
FMK-MEA	MAP4K2	MAP4K2	94	1000
FMK-MEA	MAP4K3	MAP4K3	100	1000
FMK-MEA	MAP4K4	MAP4K4	88	1000
FMK-MEA	MAP4K5	MAP4K5	86	1000
FMK-MEA	MAPKAPK2	MAPKAPK2	97	1000
FMK-MEA	MAPKAPK5	MAPKAPK5	100	1000
FMK-MEA	MARK1	MARK1	90	1000
FMK-MEA	MARK2	MARK2	81	1000
FMK-MEA	MARK3	MARK3	100	1000
FMK-MEA	MARK4	MARK4	74	1000
FMK-MEA	MAST1	MAST1	83	1000
FMK-MEA	MEK1	MAP2K1	100	1000
FMK-MEA	MEK2	MAP2K2	100	1000
FMK-MEA	MEK3	MAP2K3	97	1000
FMK-MEA	MEK4	MAP2K4	78	1000
FMK-MEA	MEK5	MAP2K5	46	1000
FMK-MEA	MEK6	MAP2K6	97	1000
FMK-MEA	MELK	MELK	95	1000
FMK-MEA	MERTK	MERTK	99	1000
FMK-MEA	MET	MET	97	1000
FMK-MEA	MET(M1250T)	MET	95	1000
FMK-MEA	MET(Y1235D)	MET	81	1000
FMK-MEA	MINK	MINK1	100	1000
FMK-MEA	MKK7	MAP2K7	78	1000
FMK-MEA	MKNK1	MKNK1	100	1000
FMK-MEA	MKNK2	MKNK2	92	1000
FMK-MEA	MLCK	MYLK3	96	1000
FMK-MEA	MLK1	MAP3K9	100	1000
FMK-MEA	MLK2	MAP3K10	77	1000
FMK-MEA	MLK3	MAP3K11	100	1000
FMK-MEA	MRCKA	CDC42BPA	92	1000
FMK-MEA	MRCKB	CDC42BPB	94	1000
FMK-MEA	MST1	STK4	94	1000
FMK-MEA	MST1R	MST1R	100	1000
FMK-MEA	MST2	STK3	95	1000
FMK-MEA	MST3	STK24	78	1000
FMK-MEA	MST4	MST4	69	1000

FMK-MEA	MTOR	FRAP1	90	1000
FMK-MEA	MUSK	MUSK	100	1000
FMK-MEA	MYLK	MYLK	100	1000
FMK-MEA	MYLK2	MYLK2	95	1000
FMK-MEA	MYLK4	MYLK4	86	1000
FMK-MEA	MYO3A	MYO3A	100	1000
FMK-MEA	MYO3B	MYO3B	79	1000
FMK-MEA	NDR1	STK38	100	1000
FMK-MEA	NDR2	STK38L	92	1000
FMK-MEA	NEK1	NEK1	100	1000
FMK-MEA	NEK11	NEK11	63	1000
FMK-MEA	NEK2	NEK2	98	1000
FMK-MEA	NEK3	NEK3	70	1000
FMK-MEA	NEK4	NEK4	100	1000
FMK-MEA	NEK5	NEK5	100	1000
FMK-MEA	NEK6	NEK6	100	1000
FMK-MEA	NEK7	NEK7	100	1000
FMK-MEA	NEK9	NEK9	99	1000
FMK-MEA	NIM1	MGC42105	100	1000
FMK-MEA	NLK	NLK	96	1000
FMK-MEA	OSR1	OXSR1	100	1000
FMK-MEA	p38-alpha	MAPK14	96	1000
FMK-MEA	p38-beta	MAPK11	90	1000
FMK-MEA	p38-delta	MAPK13	89	1000
FMK-MEA	p38-gamma	MAPK12	100	1000
FMK-MEA	PAK1	PAK1	89	1000
FMK-MEA	PAK2	PAK2	85	1000
FMK-MEA	PAK3	PAK3	100	1000
FMK-MEA	PAK4	PAK4	92	1000
FMK-MEA	PAK6	PAK6	93	1000
FMK-MEA	PAK7	PAK7	82	1000
FMK-MEA	PCTK1	PCTK1	100	1000
FMK-MEA	PCTK2	PCTK2	100	1000
FMK-MEA	PCTK3	PCTK3	100	1000
FMK-MEA	PDGFRA	PDGFRA	83	1000
FMK-MEA	PDGFRB	PDGFRB	68	1000
FMK-MEA	PDPK1	PDPK1	100	1000
FMK-MEA	PFCDPK1(P.falciparum)	PFB0815w	89	1000
FMK-MEA	PFPK5(P.falciparum)	MAL13P1.279	100	1000
FMK-MEA	PFTAIRE2	PFTK2	100	1000
FMK-MEA	PFTK1	PFTK1	100	1000
FMK-MEA	PHKG1	PHKG1	100	1000
FMK-MEA	PHKG2	PHKG2	100	1000
FMK-MEA	PIK3C2B	PIK3C2B	100	1000
FMK-MEA	PIK3C2G	PIK3C2G	92	1000
FMK-MEA	PIK3CA	PIK3CA	100	1000
FMK-MEA	PIK3CA(C420R)	PIK3CA	100	1000
FMK-MEA	PIK3CA(E542K)	PIK3CA	100	1000
FMK-MEA	PIK3CA(E545A)	PIK3CA	100	1000
FMK-MEA	PIK3CA(E545K)	PIK3CA	100	1000
FMK-MEA	PIK3CA(H1047L)	PIK3CA	100	1000
FMK-MEA	PIK3CA(H1047Y)	PIK3CA	100	1000
FMK-MEA	PIK3CA(I800L)	PIK3CA	100	1000
FMK-MEA	PIK3CA(M1043I)	PIK3CA	100	1000
FMK-MEA	PIK3CA(Q546K)	PIK3CA	100	1000
FMK-MEA	PIK3CB	PIK3CB	89	1000
FMK-MEA	PIK3CD	PIK3CD	100	1000
FMK-MEA	PIK3CG	PIK3CG	100	1000
FMK-MEA	PIK4CB	PI4KB	100	1000
FMK-MEA	PIM1	PIM1	100	1000
FMK-MEA	PIM2	PIM2	99	1000
FMK-MEA	PIM3	PIM3	100	1000
FMK-MEA	PIP5K1A	PIP5K1A	100	1000
FMK-MEA	PIP5K1C	PIP5K1C	100	1000
FMK-MEA	PIP5K2B	PIP4K2B	94	1000
FMK-MEA	PIP5K2C	PIP4K2C	100	1000

FMK-MEA	PKAC-alpha	PRKACA	100	1000
FMK-MEA	PKAC-beta	PRKACB	96	1000
FMK-MEA	PKMYT1	PKMYT1	86	1000
FMK-MEA	PKN1	PKN1	100	1000
FMK-MEA	PKN2	PKN2	94	1000
FMK-MEA	PKNB(M.tuberculosis)	pknB	100	1000
FMK-MEA	PLK1	PLK1	100	1000
FMK-MEA	PLK2	PLK2	96	1000
FMK-MEA	PLK3	PLK3	91	1000
FMK-MEA	PLK4	PLK4	100	1000
FMK-MEA	PRKCD	PRKCD	90	1000
FMK-MEA	PRKCE	PRKCE	100	1000
FMK-MEA	PRKCH	PRKCH	100	1000
FMK-MEA	PRKCI	PRKCI	75	1000
FMK-MEA	PRKCQ	PRKCQ	99	1000
FMK-MEA	PRKD1	PRKD1	100	1000
FMK-MEA	PRKD2	PRKD2	100	1000
FMK-MEA	PRKD3	PRKD3	100	1000
FMK-MEA	PRKG1	PRKG1	100	1000
FMK-MEA	PRKG2	PRKG2	98	1000
FMK-MEA	PRKR	EIF2AK2	90	1000
FMK-MEA	PRKX	PRKX	80	1000
FMK-MEA	PRP4	PRPF4B	100	1000
FMK-MEA	PYK2	PTK2B	100	1000
FMK-MEA	QSK	KIAA0999	91	1000
FMK-MEA	RAF1	RAF1	99	1000
FMK-MEA	RET	RET	88	1000
FMK-MEA	RET(M918T)	RET	100	1000
FMK-MEA	RET(V804L)	RET	100	1000
FMK-MEA	RET(V804M)	RET	100	1000
FMK-MEA	RIOK1	RIOK1	69	1000
FMK-MEA	RIOK2	RIOK2	100	1000
FMK-MEA	RIOK3	RIOK3	68	1000
FMK-MEA	RIPK1	RIPK1	100	1000
FMK-MEA	RIPK2	RIPK2	39	1000
FMK-MEA	RIPK4	RIPK4	100	1000
FMK-MEA	RIPK5	DSTKY	100	1000
FMK-MEA	ROCK1	ROCK1	98	1000
FMK-MEA	ROCK2	ROCK2	94	1000
FMK-MEA	ROS1	ROS1	100	1000
FMK-MEA	RPS6KA4(Kin.Dom.1-N-terminal)	RPS6KA4	100	1000
FMK-MEA	RPS6KA4(Kin.Dom.2-C-terminal)	RPS6KA4	100	1000
FMK-MEA	RPS6KA5(Kin.Dom.1-N-terminal)	RPS6KA5	79	1000
FMK-MEA	RPS6KA5(Kin.Dom.2-C-terminal)	RPS6KA5	98	1000
FMK-MEA	RSK1(Kin.Dom.1-N-terminal)	RPS6KA1	78	1000
FMK-MEA	RSK1(Kin.Dom.2-C-terminal)	RPS6KA1	31	1000
FMK-MEA	RSK2(Kin.Dom.1-N-terminal)	RPS6KA3	97	1000
FMK-MEA	RSK3(Kin.Dom.1-N-terminal)	RPS6KA2	83	1000
FMK-MEA	RSK3(Kin.Dom.2-C-terminal)	RPS6KA2	95	1000
FMK-MEA	RSK4(Kin.Dom.1-N-terminal)	RPS6KA6	90	1000
FMK-MEA	RSK4(Kin.Dom.2-C-terminal)	RPS6KA6	2.4	1000
FMK-MEA	S6K1	RPS6KB1	100	1000
FMK-MEA	SBK1	SBK1	98	1000
FMK-MEA	SgK110	SgK110	100	1000
FMK-MEA	SGK3	SGK3	79	1000
FMK-MEA	SIK	SIK1	98	1000
FMK-MEA	SIK2	SIK2	82	1000
FMK-MEA	SLK	SLK	100	1000
FMK-MEA	SNARK	NUAK2	96	1000
FMK-MEA	SNRK	SNRK	99	1000
FMK-MEA	SRC	SRC	98	1000
FMK-MEA	SRMS	SRMS	99	1000
FMK-MEA	SRPK1	SRPK1	100	1000
FMK-MEA	SRPK2	SRPK2	100	1000
FMK-MEA	SRPK3	SRPK3	78	1000
FMK-MEA	STK16	STK16	100	1000

FMK-MEA	STK33	STK33	100	1000
FMK-MEA	STK35	STK35	99	1000
FMK-MEA	STK36	STK36	95	1000
FMK-MEA	STK39	STK39	100	1000
FMK-MEA	SYK	SYK	96	1000
FMK-MEA	TAK1	MAP3K7	100	1000
FMK-MEA	TAOK1	TAOK1	100	1000
FMK-MEA	TAOK2	TAOK2	100	1000
FMK-MEA	TAOK3	TAOK3	100	1000
FMK-MEA	TBK1	TBK1	100	1000
FMK-MEA	TEC	TEC	100	1000
FMK-MEA	TESK1	TESK1	100	1000
FMK-MEA	TGFBR1	TGFBR1	89	1000
FMK-MEA	TGFBR2	TGFBR2	100	1000
FMK-MEA	TIE1	TIE1	100	1000
FMK-MEA	TIE2	TEK	100	1000
FMK-MEA	TLK1	TLK1	78	1000
FMK-MEA	TLK2	TLK2	95	1000
FMK-MEA	TNIK	TNIK	95	1000
FMK-MEA	TNK1	TNK1	100	1000
FMK-MEA	TNK2	TNK2	100	1000
FMK-MEA	TNNI3K	TNNI3K	89	1000
FMK-MEA	TRKA	NTRK1	82	1000
FMK-MEA	TRKB	NTRK2	74	1000
FMK-MEA	TRKC	NTRK3	91	1000
FMK-MEA	TRPM6	TRPM6	81	1000
FMK-MEA	TSSK1B	TSSK1B	100	1000
FMK-MEA	TTK	TTK	95	1000
FMK-MEA	TXK	TXK	100	1000
FMK-MEA	TYK2(JH1domain-catalytic)	TYK2	100	1000
FMK-MEA	TYK2(JH2domain-pseudokinase)	TYK2	100	1000
FMK-MEA	TYRO3	TYRO3	100	1000
FMK-MEA	ULK1	ULK1	100	1000
FMK-MEA	ULK2	ULK2	90	1000
FMK-MEA	ULK3	ULK3	99	1000
FMK-MEA	VEGFR2	KDR	85	1000
FMK-MEA	VRK2	VRK2	100	1000
FMK-MEA	WEE1	WEE1	94	1000
FMK-MEA	WEE2	WEE2	100	1000
FMK-MEA	YANK1	STK32A	94	1000
FMK-MEA	YANK2	STK32B	98	1000
FMK-MEA	YANK3	STK32C	100	1000
FMK-MEA	YES	YES1	92	1000
FMK-MEA	YSK1	STK25	100	1000
FMK-MEA	YSK4	YSK4	100	1000
FMK-MEA	ZAK	ZAK	100	1000
FMK-MEA	ZAP70	ZAP70	85	1000